Rhogocytes in larval gastropods

by

Heather Stewart
B. Sc., Simon Fraser University, 2008

A Thesis Submitted in Partial Fulfillment
of the Requirements for the Degree of

MASTER OF SCIENCE

in the Department of Biology

Supervisory Committee

Rhogocytes in larval gastropods

by

Heather Stewart
B. Sc., Simon Fraser University, 2008

Supervisory Committee

Dr. Louise R. Page, Supervisor (Department of Biology)

Dr. Patrick Gregory, Departmental Member (Department of Biology)

Dr. Patrick von Aderkas, Departmental Member (Department of Biology)

Abstract

Supervisory Committee

Dr. Louise R. Page, Supervisor (Department of Biology)

Dr. Patrick Gregory, Departmental Member (Department of Biology)

Dr. Patrick von Aderkas, Departmental Member (Department of Biology)

Rhogocytes of gastropod larvae are described from TEM images. These cells were found in the planktotrophic larvae of *Amphissa columbiana, Trichotropis cancellata, Marsenina stearnsii* (Caenogastropoda) and *Nerita melanotragus* (Neritimorpha) but not in *Siphonaria denticulata* (Heterobranchia). Previously these uniquely molluscan cells had been described in adult and direct developing larval gastropods only. Multiple functions have been proposed for rhogocytes, the most well supported being hemocyanin (HCN) synthesis. HCN was found within vacuoles of the rhogocytes of *N. melanotragus* but not within the caenogastropods. Caenogastropod rhogocytes may export HCN immediately after synthesis or they may synthesize a different protein product. Rhogocytes may be homologous with terminal cells of protonephridia, the latter used for excretion and osmoregulation. The presence of these two in gastropod larvae may be functionally related to larval body size. Large caenogastropod and neritimorph larvae have rhogocytes but not protonephridia, whereas the smaller heterobranch larvae have protonephridia but not rhogocytes.

Table of Contents

List of Figures

Acknowledgments

I would like to thank all the people who helped and supported me during this process, without you this thesis would not have been possible.

First I would like to thank my supervisor, Dr. Louise Page, for her support, guidance and patience. I would also like to thank her for the use of her specimens and for all the time she invested in sectioning them. I would like to thank the members of my committee, Dr. Patrick von Aderkas, Dr. Patrick Gregory and Dr. Melissa Frey for their helpful feedback on my thesis.

Additionally I would like to thank everyone who helped with the technical aspects of my project; the present and former aquatics facility staff, Brian Ringwood, Amy Hoare and Brendan Campbell for their help with equipment set up as well as Brent Gowen for his assistance with electron microscopy techniques.

I would also like to thank my labmates past and present, Alison Page, Alicia Donaldson, Sam Ferguson and Brenda Hookham, for their invaluable support and suggestions. In addition, I would like to thank my family and friends for their love, support and understanding during the highs and lows during my studies.

Dedication

I dedicate this thesis to my wonderful family for their years of support, understanding and patience throughout this journey.

1.0 Introduction

A rhogocyte is a distinctive cell unique to molluscs (Haszprunar, 1996). In previous studies these cells have also been referred to as pore cells, nuchal cells, Blasenzelle and Leydig's cell (Haszprunar, 1996). There are multiple traits that define rhogocytes with the most prominent being tubular or saccular invaginations of the plasma membrane spanned by cytoplasmic bars or tongues (Figures 1 and 2). It is these cytoplasmic bars that create the slit-like appearance of regions of the plasma membrane that give the cells their name ('rhogos' Gr. slit). Rhogocytes have been found in connective tissues associated with most molluscan tissues and free in the hemocoel. For example, in the vetigastropod *Megathura crenulata,* the rhogocytes have been found in connective tissue associated with the digestive gland, middle and posterior esophagus, intestine and foot (Martin *et al.*, 2011).

Rhogocytes of gastropod molluscs have been described using electron microscopy in the connective tissue of adult freshwater and terrestrial pulmonates (Sminia, 1972; Sminia *et al.*, 1972; Sminia and Boer, 1973) and adult vetigastropods (Albrecht *et al.*, 2001; Martin *et al.*, 2011). However, these distinctive cells have been described to date in only one pre-metamorphic gastropod: the encapsulated veligers of the caenogastropod, *Nucella lapillus* (Fioroni *et al.*, 1984), a species that lacks a free-living larval stage and hatches as a crawl-away juvenile. However, the majority of marine gastropods have a long-lived, feeding larval stage in the life history. Rhogocytes have not been described in the planktotrophic larval stage of any of these species.

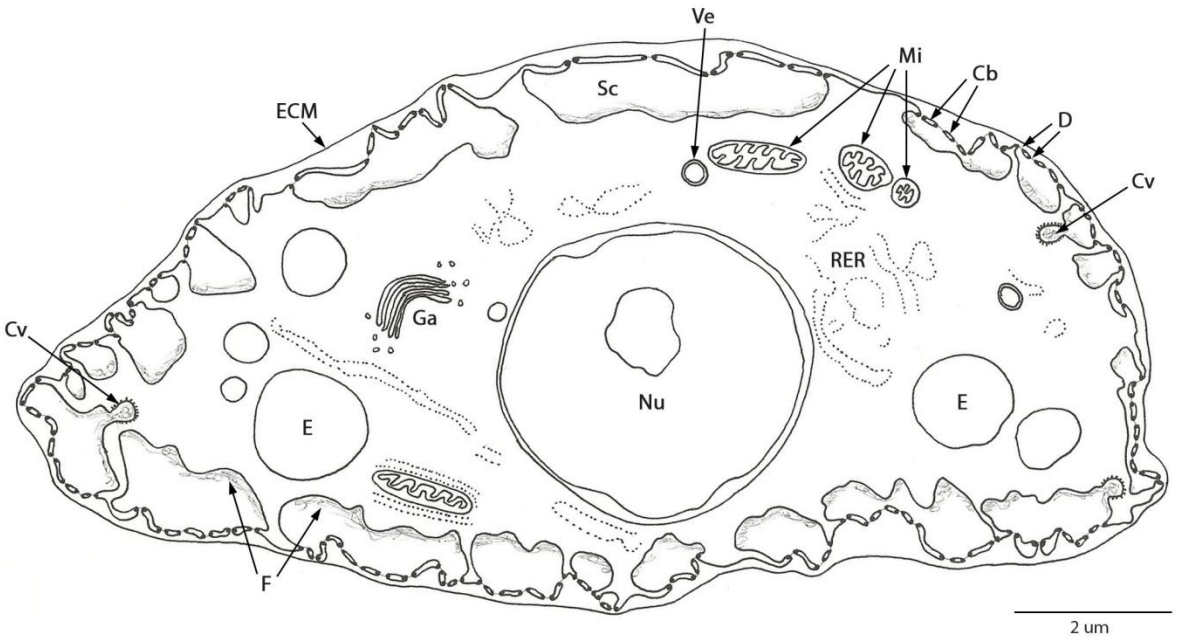

Figure 1. Drawing of a typical molluscan rhogocyte.
Cytoplasmic bars (Cb), coated vesicle (Cv), peg-like diaphragms (D), electron dense vacuoles (E), extracellular matrix (ECM), floccular material (F), Golgi apparatus (Ga), mitochondria (Mi), nucleus (Nu), rough endoplasmic reticulum (RER), subsurface cisterna (Sc), vesicle (Ve).

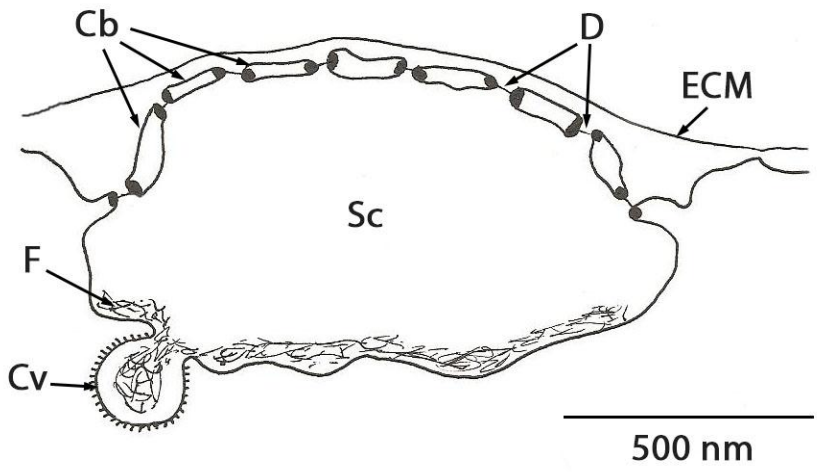

Figure 2. Typical sieve complex of a rhogocyte.

Drawing of a sieve complex and subsurface cisterna (Sc). Coated vesicle (Cv), diaphragms (D) spanning the slits between the cytoplasmic bars (Cb), extracellular matrix (ECM), floccular material (F).

1.1 Rhogocytes – review of structure and proposed functions

Between individual rhogocytes, the shape of the cell and location of the nucleus within the cell can vary. Nevertheless, rhogocytes can be easily identified during ultrastructural examination of tissue sections because of their distinctive slit openings in the plasma membrane, referred to here as the sieve complex (Figure 2). The cytoplasmic bars that form these slit openings may be joined by a delicate diaphragm across the opening (Boer and Sminia, 1976; Martin *et al.*, 2011). The entire rhogocyte is surrounded by a layer of extracellular matrix (ECM, Figure 1) (Skelding and Newell, 1975; Boer and Sminia, 1976; Jones and Bowen, 1979), often largely composed of collagen fibers (Plummer, 1966). This ECM is directly adjacent to the plasma membrane or is separated by a gap of 50 to 100 nm (Plummer, 1966). The sieve complex of rhogocytes and surrounding ECM resembles regions of protonephridial cyrtocytes and podocytes of metanephridial systems.

The area below the cytoplasmic bars is referred to as a subsurface cistern (Rivest, 1992) and often contains floccular material (Plummer, 1966; Sminia *et al.*, 1972; Jones and Bowen, 1979). There is often a complex system of rough endoplasmic reticulum (RER) within rhogocytes, although the amount of RER varies depending on the tissue in which the rhogocyte is found. The RER has been observed to have dilated cisternae containing material described as amorphous, floccular or fibrous, and it may also contain collagen and hemocyanin molecules (Plummer, 1966; Sminia *et al.*, 1972; Sminia and Boer, 1973; Skelding and Newell, 1975; Jones and Bowen, 1979; Albrecht *et al.*, 2001; Martin *et al.*, 2011). The fate of these materials is unclear.

Another characteristic of rhogocytes is the presence of vacuoles and/or vesicles exhibiting varying levels of electron density (Haszprunar, 1996; Martin *et al.*, 2011). The vacuoles serve as sites of material storage and accumulation whereas vesicles are involved in the transport or degeneration of materials as some exhibit lysosomal activity (Jones and Bowen, 1972; Martin *et al.*, 2011). The material described in these structures varies based on the function proposed for rhogocytes.

There have been many functions hypothesized for rhogocytes, such as collagen synthesis (Plummer, 1966), polysaccharide storage (Wolburg-Buchholz, 1972a; Jones and Bowen, 1979), removal of foreign particles from the blood (Wolburg-Buchholz, 1972b; Boer and Sminia, 1976), respiratory pigment recycling (Beuerlein *et al.*, 2002b) and accumulation and detoxification of metals (Marigómez *et al.*, 2002; Martin *et al.*, 2011). The most well studied function of rhogocytes is the biosynthesis of hemocyanin molecules (Sminia, 1972; Sminia *et al.*, 1972; Sminia and Boer, 1973; Skelding and Newell, 1975; Sminia and Vlugt-van Daalen, 1977; Martin *et al.*, 2011), a very large, copper-containing molecule that reversibly binds oxygen.

According to Plummer (1966) the rhogocytes found within the connective tissue capsule enveloping ganglia of the nervous system (neurolamina) in the tropical pulmonate group Achatinidae synthesize and release tropocollagen. Upon release from the cell, the tropocollagen begins to polymerize immediately forming thin fibrils of collagen that makes up the neurolamina (Plummer, 1966). Collagen production by rhogocytes has also been observed in the early life stages of another pulmonate, *Deroceras reticulatum* (Jones and Bowen, 1979). Jones and Bowen (1979) identified three types of rhogocytes, all of which synthesize collagen. Collagen fibres were

identified both within and surrounding the rhogocytes based on their diameter (Jones and Bowen, 1979). Jones and Bowen (1979) also indicated that the major function of their Type 3 and Type 3' rhogocytes was polysaccharide storage; these cells contained a large quantity of polysaccharide that occupied the majority of the rhogocyte's volume. Sminia (1972) identified polysaccharide storage as a less important, secondary function of the rhogocyte.

The sieve complex structure has led to the proposed ultrafiltration function of the rhogocyte (Boer and Sminia, 1976; Haszprunar, 1996). Rhogocytes have been shown to take up small molecules and particles from the blood, including ferritin (Sminia, 1972; Wolburg-Buchholz, 1972a; Skelding and Newell, 1975; Rivest, 1992), ^{125}I-labelled hemocyanin (Beuerlein *et al.*, 2002b), colloidal gold (diameter 15 nm) (Beuerlein *et al.*, 2002a) and trypan blue (Sminia, 1972), but they exclude ink (Sminia, 1972), larger diameter colloidal gold (Skelding and Newell, 1975), *Pseudomonas* sp. bacteria (Beuerlein *et al.*, 2002a), latex granules (110 nm) and yeast cells (Haszprunar, 1996). The uptake of substances is thought to be through endocytosis (Skelding and Newell, 1975; Boer and Sminia, 1976). The extracellular matrix could contribute to the selectivity of substances taken up by limiting the passage of larger molecules and particles into the rhogocyte (Sminia, 1972; Skelding and Newell, 1975), as it does in cyrtocytes of protonephridia and podocytes of metanephridia (Ruppert and Smith, 1988; Smith and Ruppert, 1988).

An extension of the possible role of rhogocytes in ultrafiltration processes is their potential involvement in the accumulation and detoxification of metals and the recycling of respiratory pigments. Rhogocytes have acid phosphatase activity within their

lysosomes (Sminia, 1972; Jones and Bowen, 1979), which could assist in the breakdown of endocytosed molecules. High concentrations of metals such as iron, copper and cadmium have been found in vesicles and granules within rhogocytes (Marigómez *et al.*, 2002). Vesicles within rhogocytes have also been shown using TEM to contain the respiratory pigment hemocyanin (Sminia, 1972; Sminia *et al.*, 1972; Sminia and Boer, 1973; Skelding and Newell, 1975; Hall *et al.*, 1975; Markl *et al.*, 2001; Albrecht *et al.*, 2001; Martin *et al.*, 2011). This may be evidence that these pigments are taken up by the cell through endocytosis for recycling or evidence for the synthesis of these molecules within the cell.

The function of rhogocytes that has received the most attention and has the most supporting evidence is hemocyanin synthesis. This function was proposed when studies using TEM showed evidence of molecules within the enlarged cisternae of the RER and occasionally in the subsurface cisternae of the plasma membrane that had a size and shape characteristic of hemocyanin molecules (Sminia *et al.*, 1972; Sminia and Boer, 1973; Skelding and Newell, 1975; Markl *et al.*, 2001; Martin *et al.*, 2011). Further evidence for hemocyanin biosynthesis within rhogocytes has come from reports of high concentrations of copper ions within these cells, copper being the key component of the oxygen binding site of hemocyanin (Sminia *et al.*, 1972; Marigómez *et al.*, 2002).

Immunohistochemical studies have strengthened the conclusion that rhogocytes within at least some gastropods contain hemocyanin. Experiments on the abalone, *Haliotis tuberculata*, showed that only rhogocytes were labeled with antibodies against the hemocyanin of this species (Albrecht *et al.*, 2001). Similarly, a study by Martin *et al.* (2011) showed labeling of rhogocytes in the keyhole limpet, *Megathura crenulata*, when

tissue was incubated with antibodies against hemocyanin of this species, although an earlier study by Albrecht *et al.* (2001) failed to do so. Albrecht *et al.* (2001) justified their negative result by suggesting that hemocyanin synthesis, especially in *M. crenulata*, may not occur at all times throughout the year or in uniform amounts in all tissues or cells. However, this explanation was refuted by Martin *et al.* (2011), who observed hemocyanin synthesis year round in their study on *M. crenulata*.

The presence of hemocyanin within a cell does not definitively demonstrate synthesis by the cell; the cell could serve as a storage site or be involved in breakdown and recycling of molecular components of hemocyanin. Nevertheless, the abundance of RER and Golgi complexes within the rhogocytes is consistent with a high rate of protein synthesis (Plummer, 1966; Sminia, 1972). To determine if rhogocytes do indeed synthesize hemocyanin, *in situ* hybridization has been used to demonstrate expression of hemocyanin mRNA within rhogocytes (Albrecht *et al.*, 2001; Martin *et al.*, 2011). Studies of this type have demonstrated expression of mRNA for the medically important hemocyanin isoforms within rhogocytes of the vetigastropods *H. tuberculata* and *M. crenulata* (Albrecht *et al.*, 2001; Martin *et al.*, 2011).

1.2 Hemocyanin

Hemocyanin (HCN) is the respiratory pigment found freely circulating in the hemolymph of molluscs and arthropods (Miller and van Holde, 1982; Ellerton *et al.*, 1983; van Holde, 1997). Hemocyanin is a glycoprotein utilizing copper ions at the active site of oxygen binding (Bonaventura and Bonaventura, 1980; Ellerton *et al.*, 1983; Harris

and Markl, 1999; Manubens *et al.*, 2010). Although molluscs and arthropods both use hemocyanin, the structure of this protein is different between the two phyla (Bonaventura and Bonaventura, 1980; Harris and Markl, 1999; van Holde *et al.* 2001). The following review focuses solely on molluscan hemocyanin.

The organization of hemocyanin molecules differs between classes of molluscs (Ryan *et al.,* 1985); however, they are all based on a similar hollow, cylindrical decamer structure (Hall *et al.*, 1975; Bonaventura and Bonaventura, 1980; Ryan *et al.*, 1985) that is visible with TEM. Each decamer consists of five homo-dimers and each homo-dimer is made up of two anti-parallel polypeptide chains (Markl *et al.*, 2001; Streit *et al.*, 2005). These polypeptide chains each have a molecular mass of ca. 400 kDa and contain eight different functional units (FUs) (Manubens *et al.*, 2010). Each FU contains one oxygen binding site (van Holde, 1997) consisting of two copper ions bound to three histidine residues (van Holde, 1997; Markl *et al.*, 2001; Bergmann *et al.*, 2006; Manubens *et al.*, 2010). Based on this composition, one decamer will bind 80 oxygen molecules (Wood *et al.*, 1981; van Holde 1997; Streit *et al.*, 2005) and have a diameter of ca. 35 nm.

In different molluscan classes, the HCN decamers form different quaternary arrangements. In polyplacophorans and cephalopods, the HCN decamers rarely associate with each other (Ryan et al, 1985; Bergmann *et al.*, 2006), whereas in gastropods and bivalves the decamers are typically assembled into didecamers or multidecamers (Markl *et al.*, 2001; Streit *et al.*, 2005; Bergmann *et al.*, 2006). In some gastropods, including keyhole limpets, hemocyanin exists in two isoforms, each composed of different FUs (Harris and Markl, 1999; Markl *et al.*, 2001; Streit *et al.*, 2005).

In some cephalopods the site of hemocyanin synthesis has been identified; however it is not the same structure in all cephalopods. This may hold true for gastropods as well. In the coleoids *Octopus dofleini* (Dilly and Messenger, 1972; Messenger *et al.*, 1974) and *Sepia officialinis* (Beuerlein *et al.*, 2002a, b, 2004), the branchial gland has been identified as the site of hemocyanin biosynthesis. Beuerlein *et al.* (2002a, b) describe the branchial gland of *S. officialinis* as having rhogocytes in its wall. In the nautiloids *Nautilis pompilius* and *N. macromphalus,* the enlarged terminal cells of the hepatopancreas and midgut gland tubules have been proposed as the site of hemocyanin synthesis (Ruth *et al.* 1988, 1996). Despite the difference in location, the cell structures producing the hemocyanin have striking similarities. These cells are described as triangular in shape with abundant RER, often with regions of dilated cisternae (Ruth *et al.*, 1996). They are also completely surrounded by a basal lamina containing collagen fibres (Ruth *et al.*, 1988); however, slit complexes have been identified only in cells within the branchial gland wall of *S. officialinis* (Beuerlein *et al.*, 2002a, b).

Within Gastropoda, there also appears to be variance in the location of hemocyanin synthesis. In the opisthobranch *Archidoris pseudoargus,* Schmekel and Weischer (1973) found evidence of hemocyanin within the blood gland located above the cerebropleural and pedal ganglia. The hepatopancreas has been identified as the site of hemocyanin synthesis in the caenogastropod *Concholepas concholepas*, although the cell type that is actually synthesizing the hemocyanin remains unknown (Manubens *et al.*, 2010). The rhogocyte has been deemed responsible for this process in the pulmonates *Lymnaea stagnalis* (Sminia *et al.*, 1972; Sminia and Boer, 1973), *Helix aspersa* (Sminia

and Vlugt-van Daalen, 1977), *Deroceras reticulatum* (Jones and Bowen, 1979) and *Arion hortensis* (Skelding and Newell, 1975) and in the vetigastropods *Haliotis tuberculata* (Albrecht *et al.*, 2001) and *Megathura crenulata* (Miller and van Holde, 1982; Martin *et al.*, 2011). In species in which the rhogocyte is suggested to synthesize hemocyanin, the rhogocytes are found throughout most connective tissues of the body (Streit *et al.*, 2005).

1.3 Biomedical significance of HCN

Hemocyanins from the keyhole limpet *Megathura crenulata* (KLH) (Harris and Markl, 1999; Markl *et al.*, 2001, Dolashka *et al.*, 2011), the European abalone *Haliotis tuberculata* (HtH) (Markl *et al.*, 2001), the pulmonate *Helix luconum* (β-HlH) (Dolashka *et al.*, 2011) and the caenogastropods *Concholepas concholepas* (Manubens *et al.*, 2010) and *Rapana venosa* (RvH) (Dolashka *et al.*, 2011) are biomedically important molecules. KLH and HtH have two identified isoforms (KLH-1, KLH-2 and HtH-1 and HtH-2), both of which have biomedical importance (Markl *et al.*, 1991; Söhngen *et al.*, 1997; Keller *et al.*, 1999; Lieb *et al.*, 1999).

Molluscan hemocyanin molecules elicit strong immune responses in experimental animals and clinical trials. This immune response has been attributed to the high molecular weight and carbohydrate content of the molecules (Dolashka *et al.*, 2011). Differences in the carbohydrate side chains of HCN influence the type of immune response they elicit (Harris and Markl, 1999; Dolashka *et al.*, 2011).

Hemocyanins are also used as carriers for haptens (Markl *et al.*, 2001); small natural or synthetic molecules that elicit a weak immune response on their own (Harris and Markl, 1999). The immune system produces antibodies for the HCN with the hapten

epitopes on its surface. Gradually the hemocyanin complex will be removed from the body while the immune system continues to make antibodies recognizing and targeting hapten epitopes (Dolashka *et al.*, 2011).

KLH on its own serves as a non-specific immunostimulant that has been shown to be at least comparable to other non-specific immunotherapies for the treatment of bladder carcinomas (Wirguin *et al.*, 1995) with fewer side effects (Harris and Markl, 1999). Other types of cancer are potential targets for HCN immunotherapy (Helling and Livingston, 1994; Helling *et al.*, 1995; Berard *et al.*, 2000; Schnurr *et al.*, 2001; Wandall *et al.*, 2010). KLH is being investigated as a component for generalized vaccines, for disease diagnosis including Schistosomiasis, allergy, asthma and drug addiction treatments, drug assays and immune response testing (reviewed in Harris and Markl, 1999). Gastropod hemocyanins show great potential as biomedically significant molecules, therefore continued study is important.

1.4 Possible homology between rhogocytes, cyrtocytes and podocytes

According to Haszprunar (1996) rhogocytes belong to a group of homologous cells with sieve-like structures in their plasma membranes. Other members of this cell family include the cyrtocytes of protonephridia and podocytes of metanephridial systems (Haszprunar, 1996) which are found throughout invertebrate phyla including molluscs.

1.4.1 Nephridia

The germ layer origin of nephridia has been studied and debated extensively. According to Goodrich's (1945) evolutionary model of nephridia, both protonephridia and metanephridia originate from the ectoderm or ectomesoderm. While Goodrich (1945) defined nephridia in terms of germ layer origin, Smith and Ruppert (1988; Ruppert and Smith, 1988) emphasize morphology and function in their model of nephridia.

The main function of nephridia is excretion (Goodrich, 1945), but they are also involved in osmoregulation (Raven, 1966). Nephridial function consists of two components, an initial filtration component and a subsequent reabsorption component (Ruppert and Smith, 1988; Smith and Ruppert, 1988).

Reabsorption occurs in the lumen of the nephridioduct after filtration. The nephridioducts of protonephridia and metanephridia are nearly identical (Ruppert and Smith, 1988; Smith and Ruppert, 1988). The duct cells modify the filtrate through the selective uptake of water, ions and molecules such as glucose. The modified filtrate exits the body through the nephridiopore of the aperatural cell.

1.4.2 Cyrtocytes

Filtration by protonephridia occurs via the cyrtocyte (terminal cell) that extends into the adult hemocoel or larval blastocoel. The general structure of the cyrtocyte consists of a monociliated or multiciliated cell with cytoplasmic extensions arising from the cell body to form a filtration weir (Ruppert and Smith, 1988; Smith and Ruppert,

1988; Smith, 1992; Ruppert, 1994). The cytoplasmic extensions completely surround the cilium or cilia forming a lumen that opens to the nephridioduct. The cytoplasmic extensions rest on an ECM that extends to cover the basal side of the cyrtocyte cell body (Ruppert and Smith, 1988). Filtration occurs when beating of the cilia generates negative pressure within the lumen of the cyrtocyte, which draws body fluid across the ECM and filtration weir. The ECM aids in the selectivity of what passes into the lumen by restricting passage of large macromolecules.

1.4.3 Podocytes

In metanephridial systems, filtration is performed by podocytes. Unlike cyrtocytes of protonephridia, there is very little variation between podocytes of different organisms. The filtration surface of a podocyte is formed by pedicels that extend out from the cell body (Boer and Sminia, 1976). The pedicels, and in some cases the podocyte cell body, rest on a basal ECM (Smith and Ruppert, 1988). Podocytes are pressure filtration devices; they overlay blood vessels such that the muscular action of the vessel forces water and small molecules through the ECM and pedicels. The resulting filtrate moves into the coelom and is collected by the nephridioduct.

1.4.4 Distribution of protonephridia and metanephridia in larval gastropods

Based on their studies on polychaete excretion, Smith and Ruppert (1988; Ruppert and Smith, 1988) defined a general rule for the distribution of protonephridia and

metanephridia that holds true outside Annelida. The rule states that organisms with a blood vascular system (BVS) have metanephridia, whereas those without a BVS have protonephridia.

Most adult molluscs, including gastropods, possess a BVS and utilize metanephridia as adults. Larval molluscs typically have protonephridia for osmoregulation and excretion, but they replace these with metanephridia at metamorphosis or during the juvenile stage (Baeumler *et al*., 2011). However, different groups of gastropods show differences in when they convert from protonephridia to metanephridia. Heterobranch larvae typically have protonephridia throughout the larval stage (Bartolomaeus, 1989; Page, 1994), but caenogastropods have protonephridia only during encapsulated embryonic development. At the time of hatching, caenogastropods replace protonephridia with a metanephridium (Ruthensteiner and Schaefer, 1991). They are replaced by metanephridia that persist through metamorphosis (Fahrner and Haszprunar, 2001; Baeumler *et al.*, 2011).

During early intracapsular development of direct developing caenogastropods a pair of larval kidneys, which are protonephridial derivatives (Ruthensteiner and Schaefer, 1991; Rivest, 1992), have been described (Raven, 1966; Ruthensteiner and Schaefer, 1991; Rivest, 1992; Fretter and Graham, 1994). The larval kidneys are a pair of protruding structures, laterally located in the region posterior to the velum, which are completely reabsorbed prior to hatching (Ruthensteiner and Schaefer, 1991; Rivest, 1992). A component of the larval kidneys described by Rivest (1992) was interpreted by Haszprunar (1996) as an intermediate between rhogocytes and cyrtocytes, however I

interpret Rivest's finding as evidence that the larval kidneys are highly derived nephridioducts that have become specialized for uptake of intracapsular albumen.

1.5 Purpose of this thesis

The objective of this thesis was to use transmission electron microscopy (TEM) to attempt to identify rhogocytes within planktotrophic larvae of two major gastropod clades, Caenogastropoda and Neritimorpha. Rhogocytes were located within larvae of three caenogastropod species, each belonging to a different family, and one neritimorph species. The study of rhogocytes is important as these cells have been identified as a site of synthesis of the respiratory pigment hemocyanin. Using TEM, I compared larval rhogocytes to the cyrtocytes of protonephridia of the larval heterobranch, *Siphonaria denticulata*, with a view to providing evidence of homology between rhogocytes and cyrtocytes. As rhogocytes of adult pulmonates and vetigastropods have been shown to contain hemocyanin molecules (Sminia, 1972; Sminia and Boer, 1973; Albrecht *et al.*, 2001) I looked for evidence of hemocyanin molecules within the larval rhogocytes using TEM.

The majority of caenogastropods have a feeding larval stage during their early development; however no feeding larvae have been examined for the presence of rhogocytes. The three caenogastropods included in this study are *Amphissa columbiana* (Neogastropoda; Columbellidae), *Marsenina stearnsii* (Velutinidae) and *Trichotropis cancellata* (Capulidae). These species all experience extended periods of time as planktonic, feeding larvae called veligers, after undergoing intracapsular embryonic development to reach the veliger stage.

Amphissa columbiana is an intertidal, scavenging species that undergoes internal fertilization and the female lays egg capsules. Each egg capsule can contain up to 60 embryos (Seavy, 1977; Strathmann, 1987), all of which have the potential to develop into a functional individual. *Amphissa columbiana* veligers hatch after approximately 72 days at 10°C (Seavy, 1977) or four to six weeks at 16°C (Page and Parries, 2000) to become planktotrophic veligers feeding on microalgae.

Marsenina stearnsii is a low rocky intertidal species that feeds on colonial ascidians (Gittenberger, 2007). Females embed their egg capsules, containing several hundred embryos, in the colonial ascidian *Tridemnun opacum* (Page, 2002). Embryogenesis lasts approximately 28-35 days in laboratory conditions at 10°C, at which point veligers hatch and begin to feed on microalgae in the plankton (Page, 2002).

Adults of *T. cancellata* are suspension feeding caenogastropods that can also be kleptoparasites of tube-dwelling polychaetes that live in the shallow subtidal zone (Yonge, 1962; Iyengar, 2005). *Trichotropis cancellata* is protandric (Yonge, 1962; Iyengar, 2005) and reproduces in the winter months, at which point they leave their hosts to mate (Iyengar, 2005). At 10°C, approximately two months after deposition of the egg capsule, planktotrophic veliger larvae hatch (Parries and Page, 2003).

Neritimorpha is another major clade of gastropods. Like caenogastropods, many aquatic neritimorphs also have planktotrophic larvae (Bandel, 1982; Kano *et al.*, 2002; Kano, 2006). Neritimorphs exist in ecosystems throughout the world in a range of marine, freshwater and terrestrial habitats, although they exhibit greatest diversity and abundance in tropical and semi-tropical latitudes (Kano *et al.*, 2002; Kano, 2006; Lindberg, 2008).

In this study the neritimorph investigated was *Nerita melanotragus* (Neritidae), a rocky intertidal species common in Australia. Adults deposit lens-shaped egg capsules on the rocky substratum of their habitat (Tan and Lee, 2009). Embryogenesis occurs within the egg capsules and a specific cue may be required to induce hatching of planktotrophic veligers (Lesoway and Page, 2008). Without the appropriate cue to trigger hatching, veligers can remain within the egg capsule for extended periods of time (Page, unpublished observations). Once released from their egg capsule, these veligers require an extended period of feeding in the plankton prior to metamorphosis and settlement (Lesoway and Page, 2008).

Heterobranchia is a large clade of gastropods that also has aquatic species with a planktotrophic larval stage (Ponder and Lindberg, 1997). Heterobranchs inhabit marine, freshwater and terrestrial environments. The heterobranch included in this study is the mid-intertidal false limpet, *Siphonaria denticulata*. This is a common rocky intertidal species in Australia where they graze macroalgae (Iveša *et al.*, 2010). Adults can spawn up to once every two weeks during the summer months (Creese, 1980) depositing egg ribbons on the rocky substratum (Moreira *et al.*, 2006). The frequency of spawning and size of egg ribbons however depends on adult body size (Creese, 1980).

2.0 Materials and Methods

2.1 Collection and culture of embryos and larvae

Amphissa columbiana, Trichotropis cancellata and *Marsenina stearnsii* were collected from sites around the southern tip of Vancouver Island (Canada) or San Juan Island (Washington) and maintained in the recirculating seawater system at the University of Victoria. *Nerita melanotragus* and *Siphonaria denticulata* were collected from the rocky intertidal zone bordering Balmoral Bay within Sydney Harbour, Australia.

Adult *T. cancellata* were collected by SCUBA divers from Shady Cove, San Juan Island and Ten Mile Point, Vancouver Island. Adults were transported to UVic and maintained at 10°C in glass aquaria within the University of Victoria's recirculating seawater system. Egg capsules laid by adults on the aquarium walls were removed with a razor blade and placed in glass beakers of continuously aerated seawater at 10-11°C. The water was replaced in the beakers every one to two days until hatching.

Egg capsules of *M. stearnsii* were found embedded in a colony of the ascidian, *Tridemnun opacum,* in the low rocky intertidal region of Margaret's Bay, Vancouver Island. The capsules and the colony were collected and treated in the same manner as the egg capsules of *A. columbiana* and *T. cancellata*.

Pebbles with attached egg capsules of *N. melanotragus* and egg masses of *S. denticulata* were collected and maintained in field collected seawater at 20-23°C. *Siphonaria denticulata* egg masses were kept in 500 ml bowls of seawater, changed

daily, whereas pebbles with *N. melanotragus* egg capsules were maintained in a 20 l aquarium with an activated charcoal filter under constant aeration.

Hatched larvae were cultured in 500 ml of coarsely filtered seawater (Millipore, Bedford, MA) at an initial density of 0.5 larvae/ml for *A. columbiana* and *T. cancellata* at 16°C and 0.12-0.2 larvae/ml for *M. stearnsii* at 12°C. Larvae were transferred to fresh water every two to three days by gentle sieving through Nitex mesh and pipetting. To prevent bacterial growth, the antibiotics Streptomycin sulfate (0.05 mg/ml) and Penicillin G (0.06mg /ml) (Sigma Chemicals, St. Louis, MO) were added occasionally to the cultures at the time of water changes.

Hatched *S. denticulata* larvae, pooled from three or four egg masses, were transferred to 0.6 l glass beakers for culture at an initial density of 2 larvae/ml. Cultures were maintained at 20-23°C and culture water was changed daily. Larvae of *N. melanotragus* were not released naturally from their capsule; therefore the capsules were artificially opened. Larvae from three or four capsules were pooled and those showing vigorous swimming and ingestion of microalgae were cultured at an initial density of 0.3 larvae/ml in 1 l glass beakers (20-23°C).

At the time of water changes, the larval cultures were also provided with microalgae as food for the larvae. The microalgae were cultured in Provasoli's ES Enrichment medium to feed *A. columbiana, T. cancellata* and *M. stearnsii* and in Guillard's f/2 medium without silicates for feeding *N. melanotragus* and *S. denticulata*, at room temperature under constant illumination. Prior to being added to the larval cultures, microalgae were centrifuged and resuspended in coarse filtered seawater. The concentration of the resuspended microalgae was determined using a hemocytometer and

the volume required to achieve feeding density was calculated. *Amphissa columbiana* larvae were fed *Isochrysis galbana* (Carolina Biological Supply, Gladstone, OR) at a concentration of 0.5 to 1 x 10^5 algal cells/ml based on larval size. Cultures of *T. cancellata* were fed *I. galbana* alone or a combination of *I. galbana*, *Pavlova lutheri* and *Rhodomonas salina* (Provasoli-Guillard Culture Centre for Marine Phytoplankton, Bigelow Laboratories, Boothbay, ME) at a density of 10^5 algal cells/ml. *Marsenina stearnsii* were fed the same combination and density of *I. galbana*, *P. lutheri* and *R. salina* as *T. cancellata.* Larvae of *N. melanotragus* and *S. denticulata* were fed a 1:1 mixture of *Isochrysis* sp. (TIso strain) and *P. lutheri* (CSIRO Microalgae Supply Service, Tasmania, Australia). Cultures of *N. melanotragus* were fed microalgae at a density of 4 x 10^4 algal cells/ml and *S. denticulata* were fed 2 x 10^4 algal cells/ml of the microalgal mixture.

Larvae were raised to different ages; *A. columbiana* was raised to 18 days post hatching (dph), *T. cancellata* to 3 dph and *M. stearnsii* to 13 dph, at which point they were fixed. *Siphonaria denticulata* were fixed within hours of hatching. Larval *N. melanotragus* were fixed immediately after artificial release from the egg capsule after they exhibited swimming and feeding activity.

2.2 Preparation of histological sections and transmission electron microscopy

The following larvae were fixed for examination by transmission electron microscopy: *Amphissa columbiana* at 18 days post-hatching (dph), *Trichotropis*

cancellata at 3 dph, *Marsenina stearnsii* at 13 dph, *Siphonaria denticulata* at hatching, and *Nerita melanotragus* at the time of artificial release from the egg capsule.

Prior to fixation, larvae were anaesthetized in artificial seawater with an elevated concentration of Mg^{2+} and a reduced concentration of Ca^{2+} (MgSW) (Audesirk and Audesirk, 1980). Larvae were placed in 8 ml vials containing 75% seawater and 25% MgSW at 10°C. The solution was gradually increased to full strength MgSW over two to three hours. The volume of MgSW in the vial was reduced to approximately 2 ml and three drops of a saturated solution of chlorobutanol in seawater were added to the vial every 1.5 min for 9 to 15 min. The anaesthetizing fluid was then replaced with primary fixative. The primary fixative consisted of 2.5% glutaraldehyde in Millonig's phosphate buffer (pH 7.6; 0.2 M) and 0.14 M NaCl (Cloney and Florey, 1968). Larvae were stored in primary fixative at 6-10°C for up to several weeks.

After fixation, larvae were decalcified for up to 12 h in a 1:1 mixture of primary fixative and 10% ethylene diaminotetracetic acid (disodium salt). The decalcified larvae were then rinsed four times for 10 min each in 2.5% sodium bicarbonate buffer (pH 7.2). Specimens were post fixed for one hour in 2% osmium tetroxide in 1.25% sodium bicarbonate buffer (pH 7.2). A graded ethanol series was used to dehydrate *A. columbiana, T. cancellata* and *M. stearnsii* specimens and a graded acetone series was used to dehydrate *N. melanotragus* and *S. denticulata* specimens. When ethanol was used for dehydration, propylene oxide was subsequently used as a transitional agent. The specimens were embedded in epoxy resin for sectioning: *A. columbiana* and *T. cancellata* in Epon resin 828, *M. stearnsii* in Taab 812 (Marivac), *N. melanotragus* and *S. denticulata* in Procure 812 (ProSciTech).

Thick sections (1 µm) from multiple larvae of each species were stained with a mixture of methylene blue and azure II (Richardson *et al.*, 1960) for light microscopy. Sections were examined for the presence of rhogocytes with a Zeiss Axioskop compound microscope and photographed using a Retiga 200T digital camera operated by QCapture Pro 5.1 (QImaging). Ultrathin sections of one specimen of each species were cut for TEM using a Diatome diamond knife on a Leica Ultracut UCT microtome. Sections were transferred to copper mesh grids and stained with a saturated aqueous solution of uranyl acetate for one hour and 0.2% lead citrate for seven minutes. Stained sections were examined with a Hitachi H-7000 transmission electron microscope. Brightness and contrast of images were adjusted using Adobe Photoshop CS6.

3.0 Results

Rhogocytes were observed in thick sections of *Amphissa columbiana*, *Marsenina stearnsii*, *Trichotropis cancellata* and *Nerita melanotragus*. Ultrathin sections from one specimen of each species were observed with TEM and hemocyanin was visible only in the rhogocytes of *N. melanotragus*.

3.1 Ultrastructure of *Amphissa columbiana* rhogocytes

Larvae of *A. columbiana* were fixed at 18 dph. Frontal sections through larvae at this stage of development revealed two rhogocytes at the level of the statocysts, one on each side of the esophagus (Figure 3). The rhogocytes were irregularly shaped, so that single sections often included multiple profiles through a single rhogocyte.

Rhogocytes of *A. columbiana* had very large subsurface cisternae covered by sieve complexes that protruded from the surface of the cell (Figures 4 and 5). The slits between the cytoplasmic bars of the sieve complex were uniform in width (mean ± standard deviation; 14.1 ± 4.0 nm, n = 25) but the cytoplasmic bars had variable widths ranging from 100 nm to 270 nm. In cross section, the periphery of each cytoplasmic bar had a small region of higher electron density than the central region of the bar (Figure 5). This was more obvious in obliquely sectioned sieve complexes as there was a band of higher electron density at the edge of the cytoplasmic bars along their entire length (Figure 6). Oblique sections also showed delicate, regularly-spaced fibrils extending across slits between cytoplasmic bars (Figure 6). These fibrils were present in all species

Figure 3. Location of rhogocytes in *Amphissa columbiana*.

Light micrograph of a frontal section of *Amphissa columbiana* at 18 days post-hatching showing a rhogocyte (R) dorsal to the statocyst (St). In more posterior sections a second rhogocyte was visible on the opposite side of the esophagus (Es) dorsal to the statocyst. Mantle cavity (Mc), statolith (Sl).

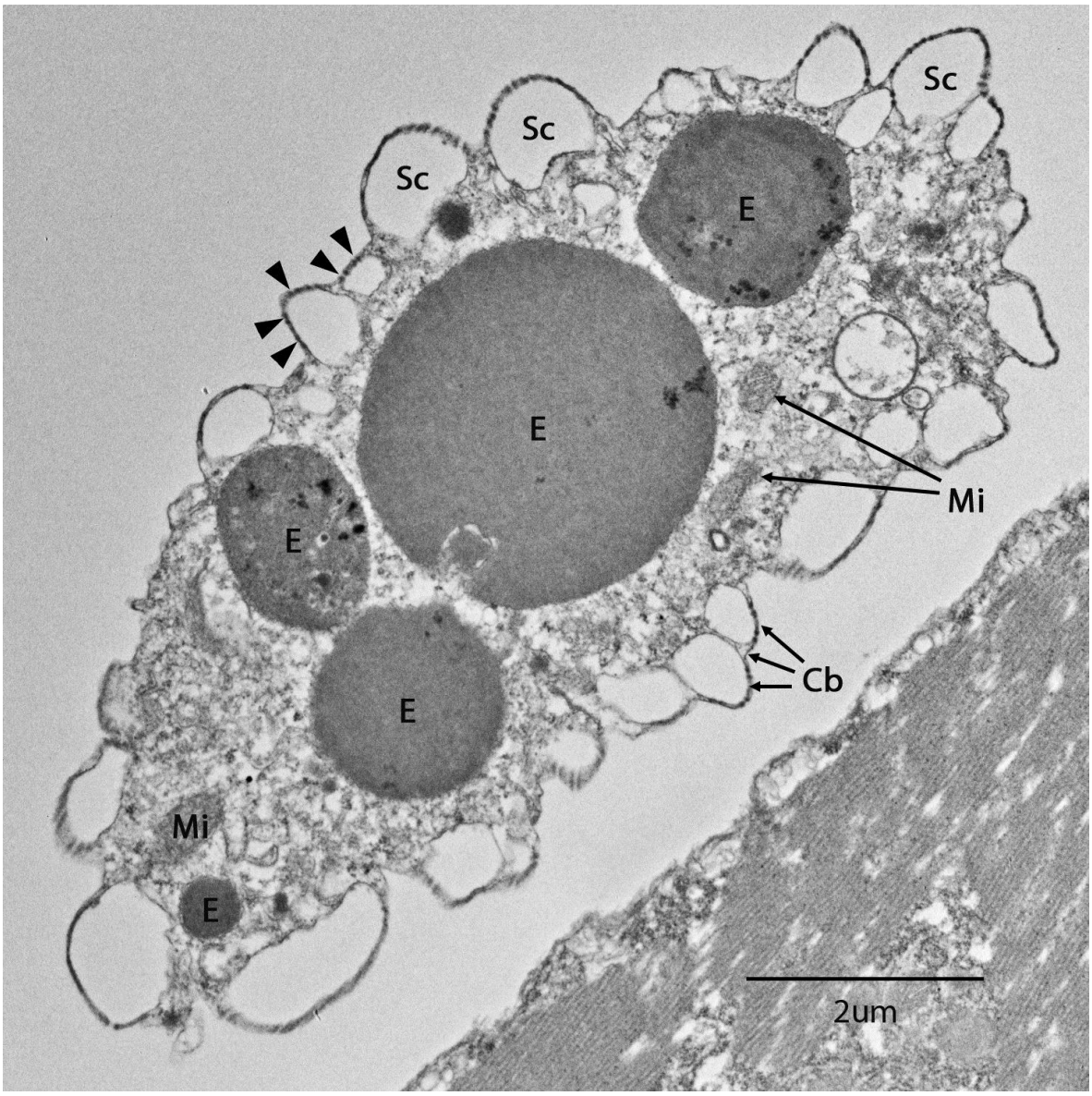

Figure 4. *Amphissa columbiana* rhogocyte.

Rhogocyte of an *Amphissa columbiana* larva at 18 days post-hatching (TEM). Cytoplasmic bars (Cb) separated by slits (arrowheads), electron dense vacuoles (E), mitochondria (Mi).

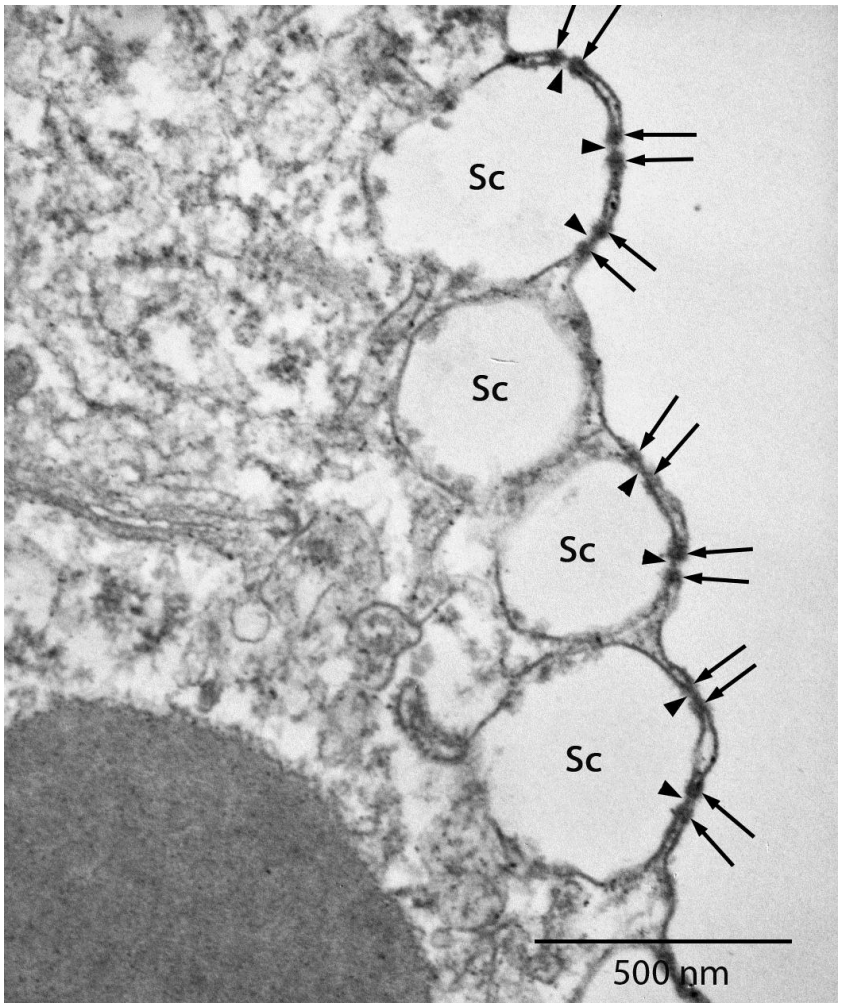

Figure 5. Sieve complexes in a rhogocyte of *Amphissa columbiana*.

TEM image of a cross section of the sieve complexes of an *Amphissa columbiana* rhogocyte (18 dph). The subsurface cisternae (Sc) are covered by cytoplasmic bars with electron dense regions on their periphery (arrows). The slits between the bars are spanned by thin, discontinuous diaphragms (arrowheads).

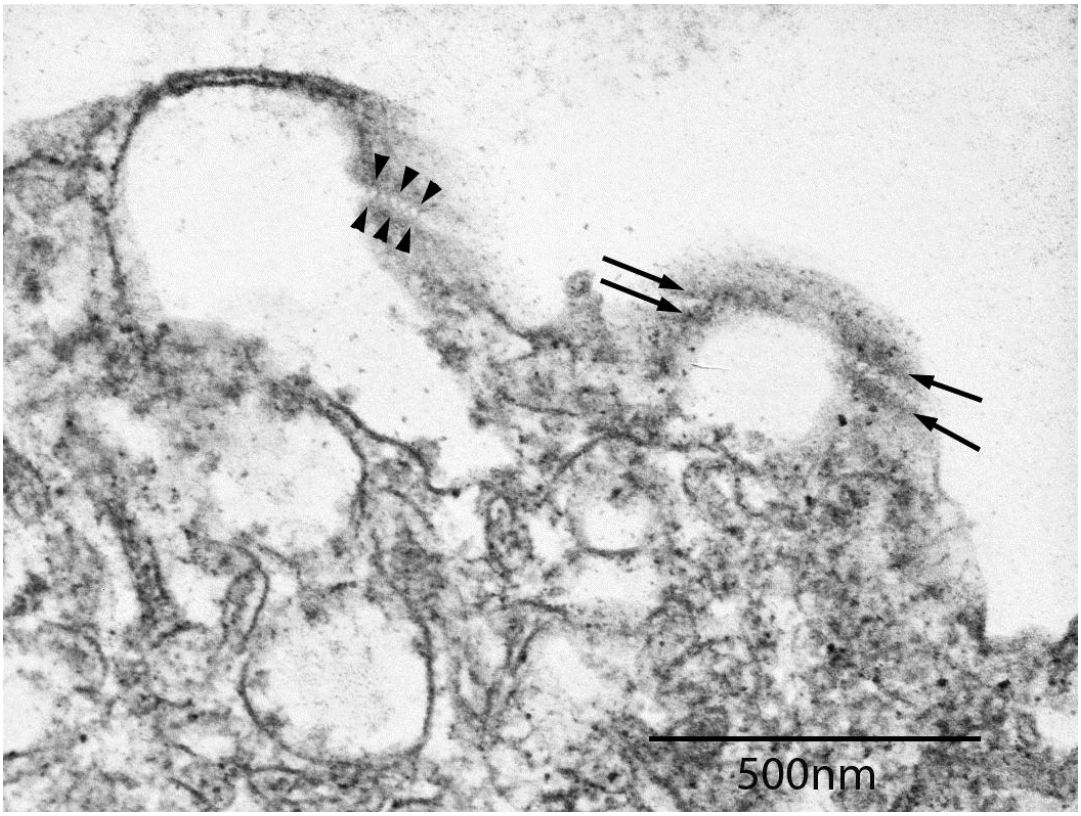

Figure 6. Slits of sieve complexes in an *Amphissa columbiana* rhogocyte. Obliquely sectioned sieve complexes of a rhogocyte in *Amphissa columbiana* (TEM, 18 dph). Electron dense regions along the periphery of the cytoplasmic bars (arrows) extend down their entire length. Peg-like, discontinuous projections extend into the slit opening between two bars (arrowheads).

studied and appeared to be a discontinuous diaphragm or peg system as described by Boer and Sminia (1976).

The sieve complexes of the rhogocytes in larvae of *A. columbiana* occupied the majority of the peripheral surface area of the cell (Figure 4). There were only small regions of the cell perimeter where there were not sieve complexes. In some locations, sieve complexes and subsurface cisternae were stacked, with the slits of the innermost complex opening into the cistern of the adjacent sieve complex (Figure 7).

Coated vesicles with their membrane confluent with the membrane lining the base of subsurface cisternae were frequently seen (Figure 8). It is unclear if these vesicles were in the process of endocytosis or exocytosis, but they did contain amorphous, floccular material similar to that in the subsurface cisternae (Figure 8). There were also coated vesicles containing floccular material that were free within the cytoplasm, but their origin and fate was unclear. Rhogocytes contained large, round vacuoles containing a material of uniform electron density, although peripheral areas of the vacuole occasionally included material of differing electron density. In one instance, an electron dense granule appeared to be engulfing material of the same electron density from the cytoplasm (Figure 9).

Rough endoplasmic reticulum was present in small amounts throughout the cytoplasm. There were no obviously expanded regions of RER. Multiple mitochondria and Golgi apparatuses throughout the cytoplasm of rhogocytes in larvae of *A. columbiana* indicated that these cells were synthetically active.

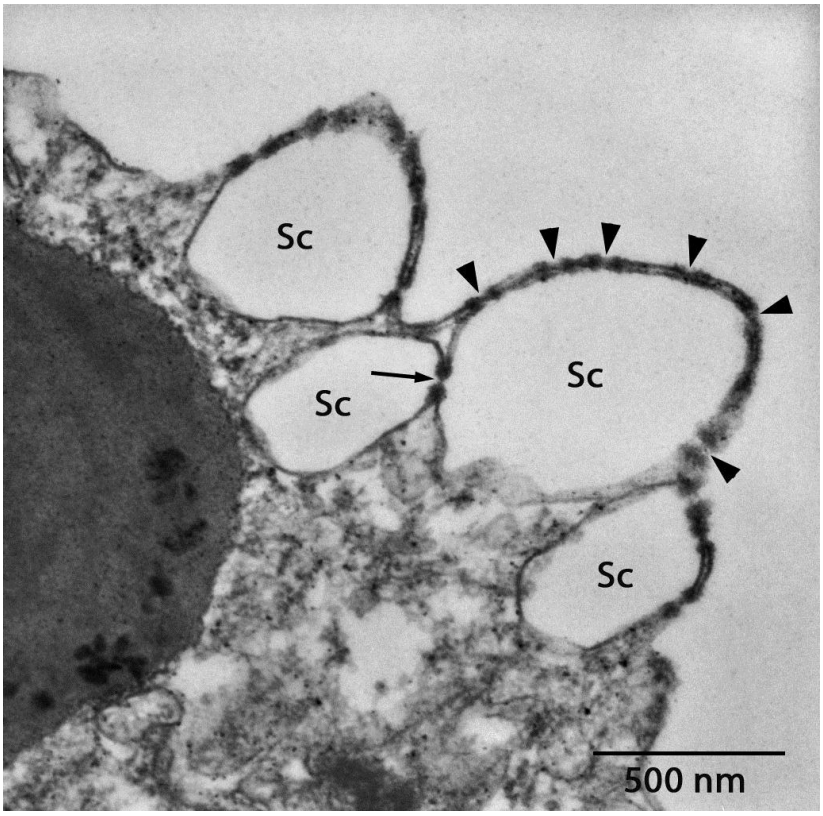

Figure 7. Stacked sieve complexes of an *Amphissa columbiana* rhogocyte.

Stacked sieve complexes in an *Amphissa columbiana* rhogocyte (TEM, 18 dph). The slit opening (arrow) of the interior-most sieve complex opens into the subsurface cisterna of the adjacent sieve complex. The slits of the outer-most sieve complex (arrowheads) open outside of the cell. Subsurface cisternae (Sc).

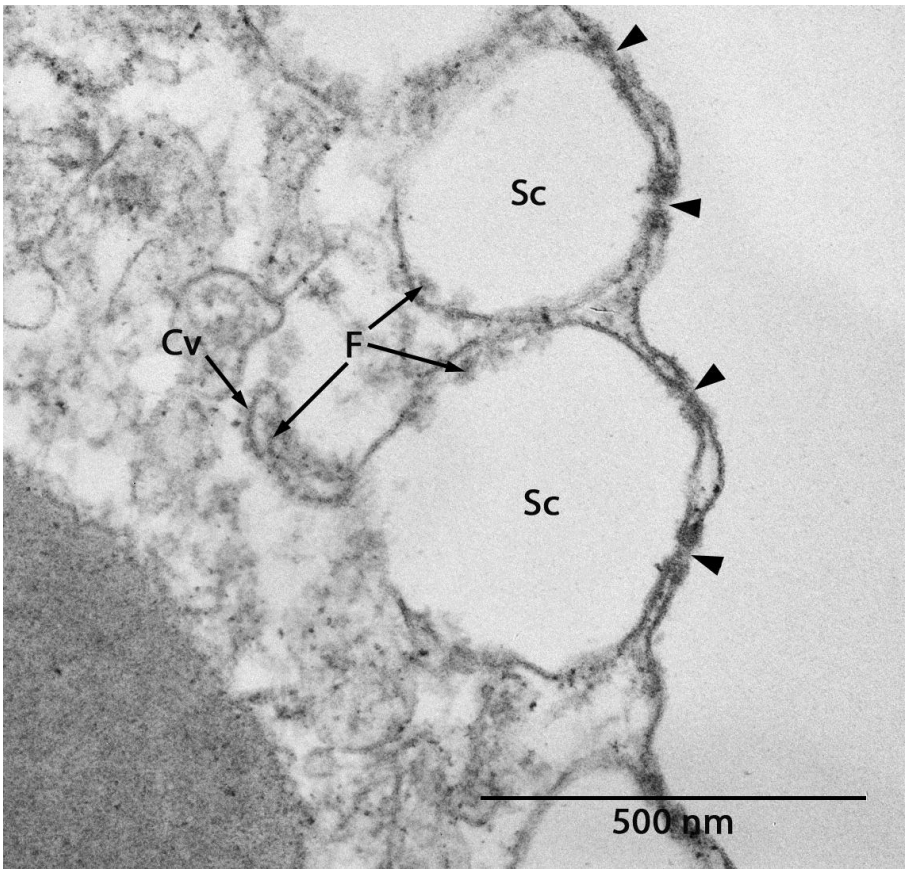

Figure 8. Coated vesicle in an *Amphissa columbiana* rhogocyte.

A coated vesicle (Cv) continuous with the base of a subsurface cistern (Sc) of a sieve complex of an *Amphissa columbiana* rhogocyte (TEM, 18 dph). Floccular material (F) is contained within the vesicle and at the base of the subsurface cistern. Slits of the sieve complex (arrowheads).

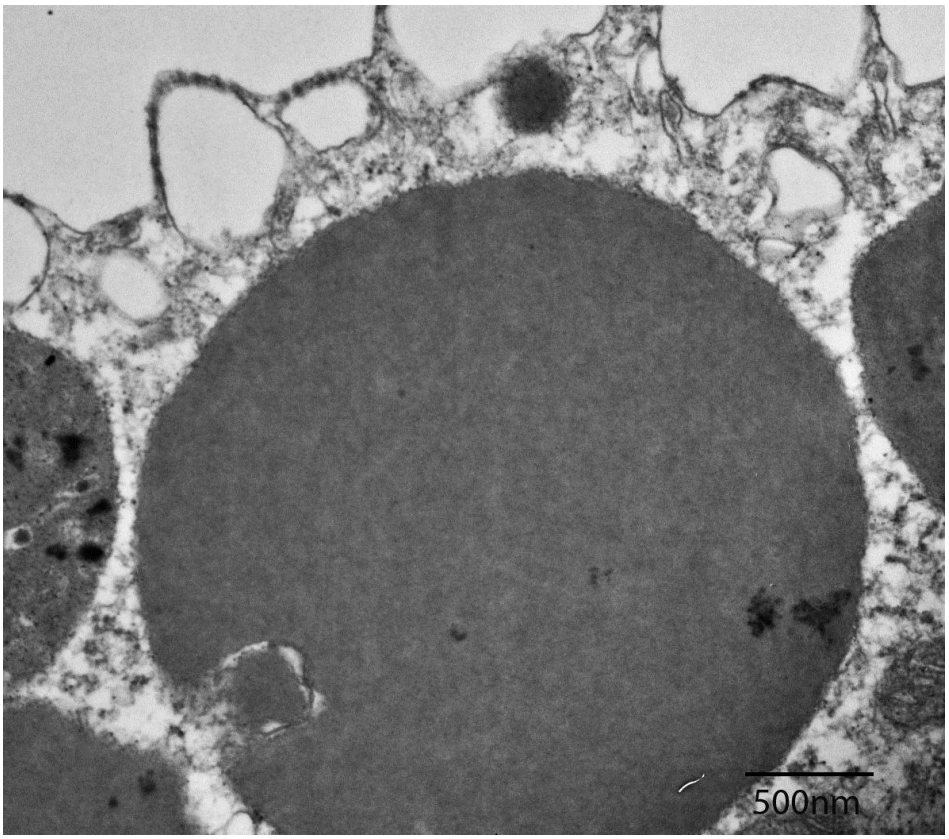

Figure 9. Electron dense vacuole in an *Amphissa columbiana* rhogocyte.

An electron dense vacuole, in the rhogocyte of *Amphissa columbiana*, engulfing an electron dense region from the cytoplasm (TEM, 18 dph).

All previous descriptions of rhogocytes have included an extracellular matrix surrounding the cell. However, there was no evidence of an ECM surrounding the rhogocytes of larval *A. columbiana* examined in this study.

3.2 Ultrastructure of *Marsenina stearnsii* rhogocytes

Larvae of *M. stearnsii* were fixed and sectioned at 13 dph. In frontal sections cut slightly posterior to the statocysts, two rhogocytes were obvious ventral to the esophagus, with one on each side of its midline (Figure 10). Rhogocytes were identified by their characteristic sieve complexes and large vacuoles containing material of medium electron density (Figure 11).

The rhogocytes in *M. stearnsii* were irregularly shaped, similar to those in *A. columbiana*. The sieve complexes covered the majority of the cell periphery. The subsurface cisternae were shallow and covered large spans without interruption (Figure 12). The slits (diameter 18.8 ± 3.4 nm, n = 25) were regularly spaced over the subsurface cisternae with narrow cytoplasmic bars between them. The cytoplasmic bars, as described for *A. columbiana*, had electron dense bands at their edges that extended down their entire length.

The basal areas of the subsurface cisternae frequently had long, thin channels extending into the cytoplasm (Figure 13). Coated vesicles were often attached to the blind ends of these channels. These channels contained floccular material that was also seen at the base of the cisternae and in the coated vesicles that were contiguous with them. Coated and uncoated vesicles were also free in the cytoplasm, both containing floccular material.

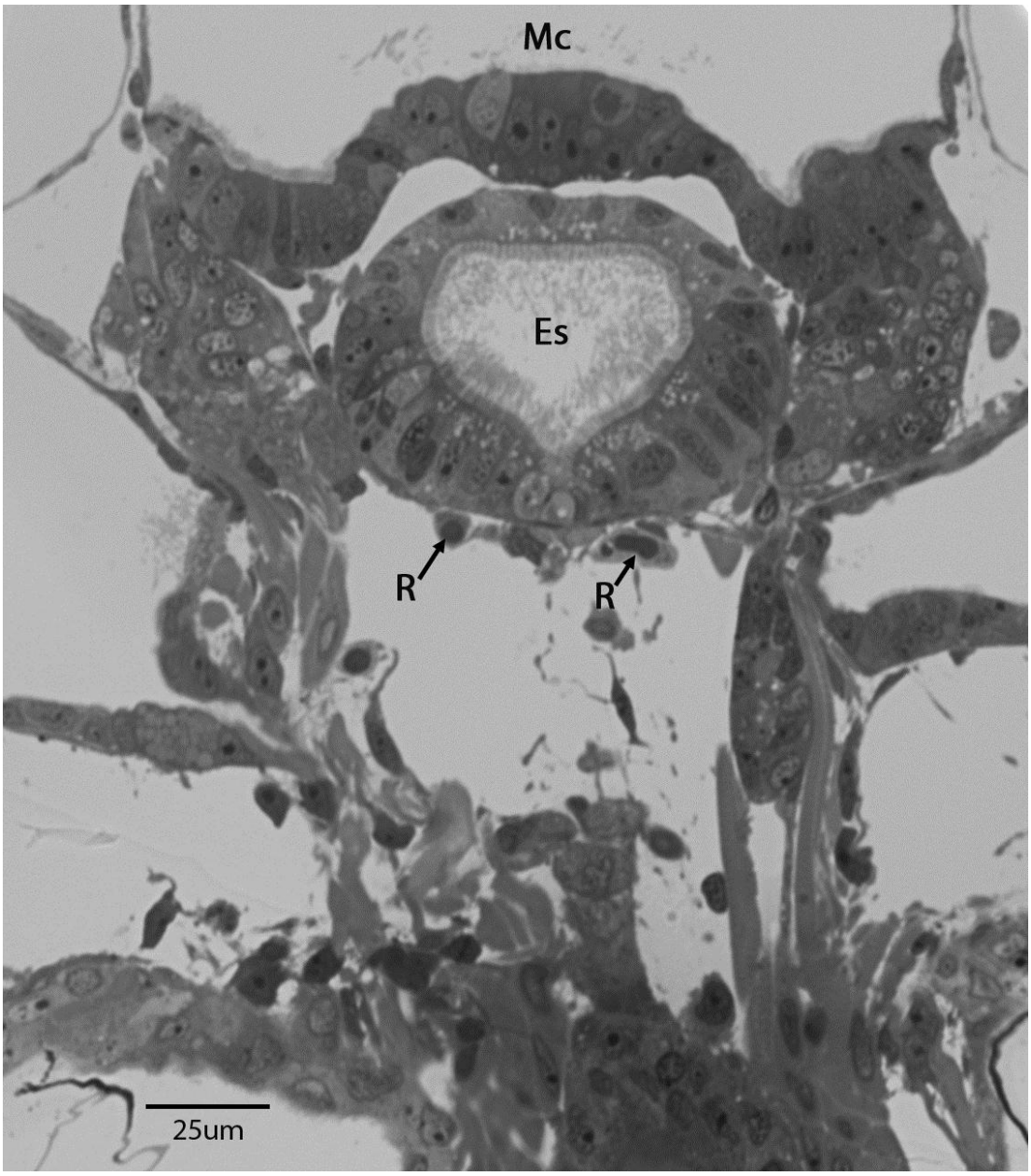

Figure 10. Location of rhogocytes in *Marsenina stearnsii.*

Light micrograph of a frontal section of a 13 dph *Marsenina stearnsii* larva. Section was taken posterior to the statocysts. A pair of rhogocytes (R) is present ventral to the esophagus (Es) with one on each side of the esophagus midline. Mantle cavity (Mc).

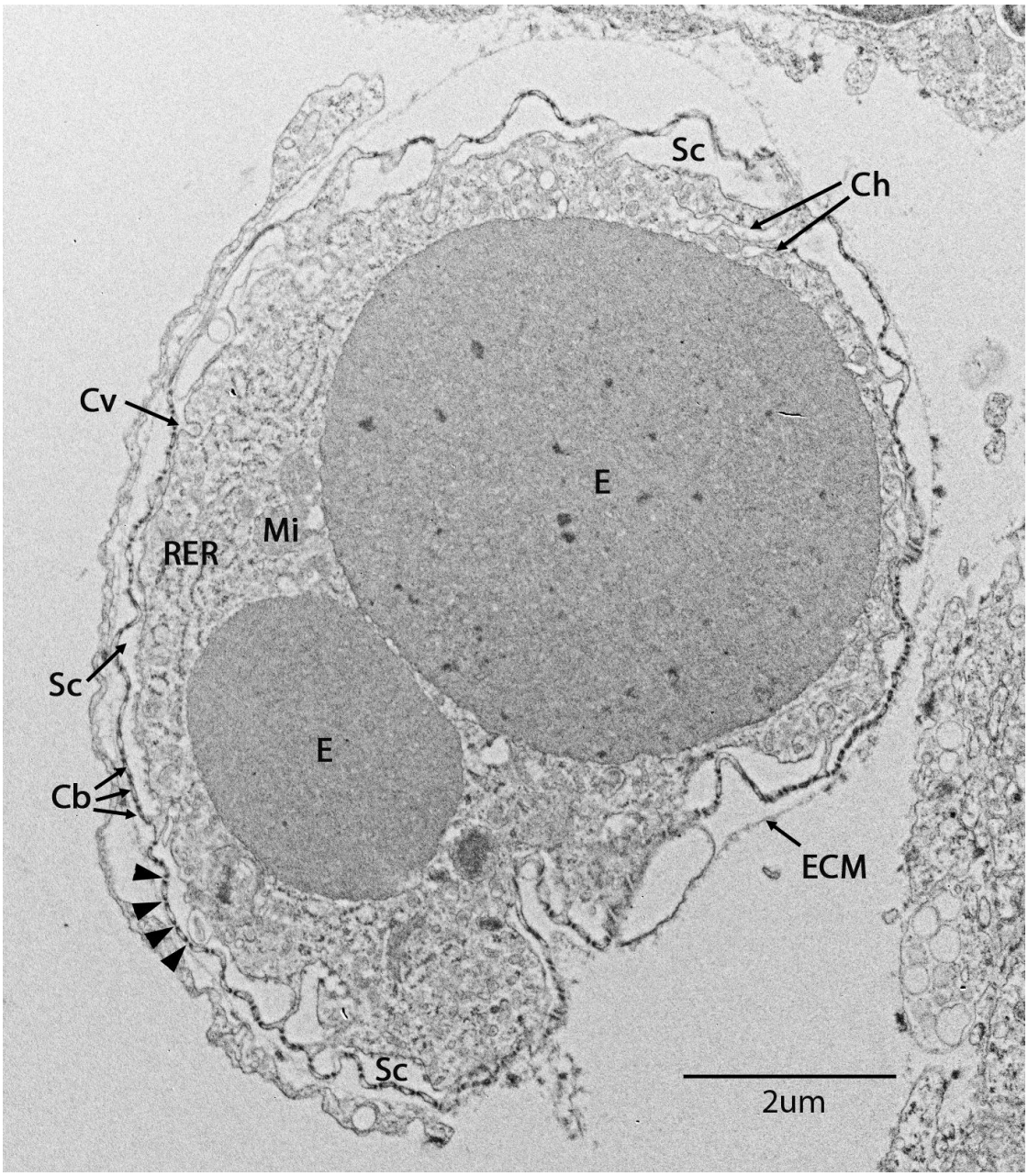

Figure 11. Rhogocyte of *Marsenina stearnsii*.

TEM image of a rhogocyte in a frontal section of a *Marsenina stearnsii* larva (13 dph). Cytoplasmic bars (Cb) with slits between them (arrowheads), channels (Ch) branching off of the base of the subsurface cisternae (Sc), coated vesicles (Cv), moderately electron dense vacuoles (E), extracellular matrix (ECM), mitochondrion (Mi), rough endoplasmic reticulum (RER).

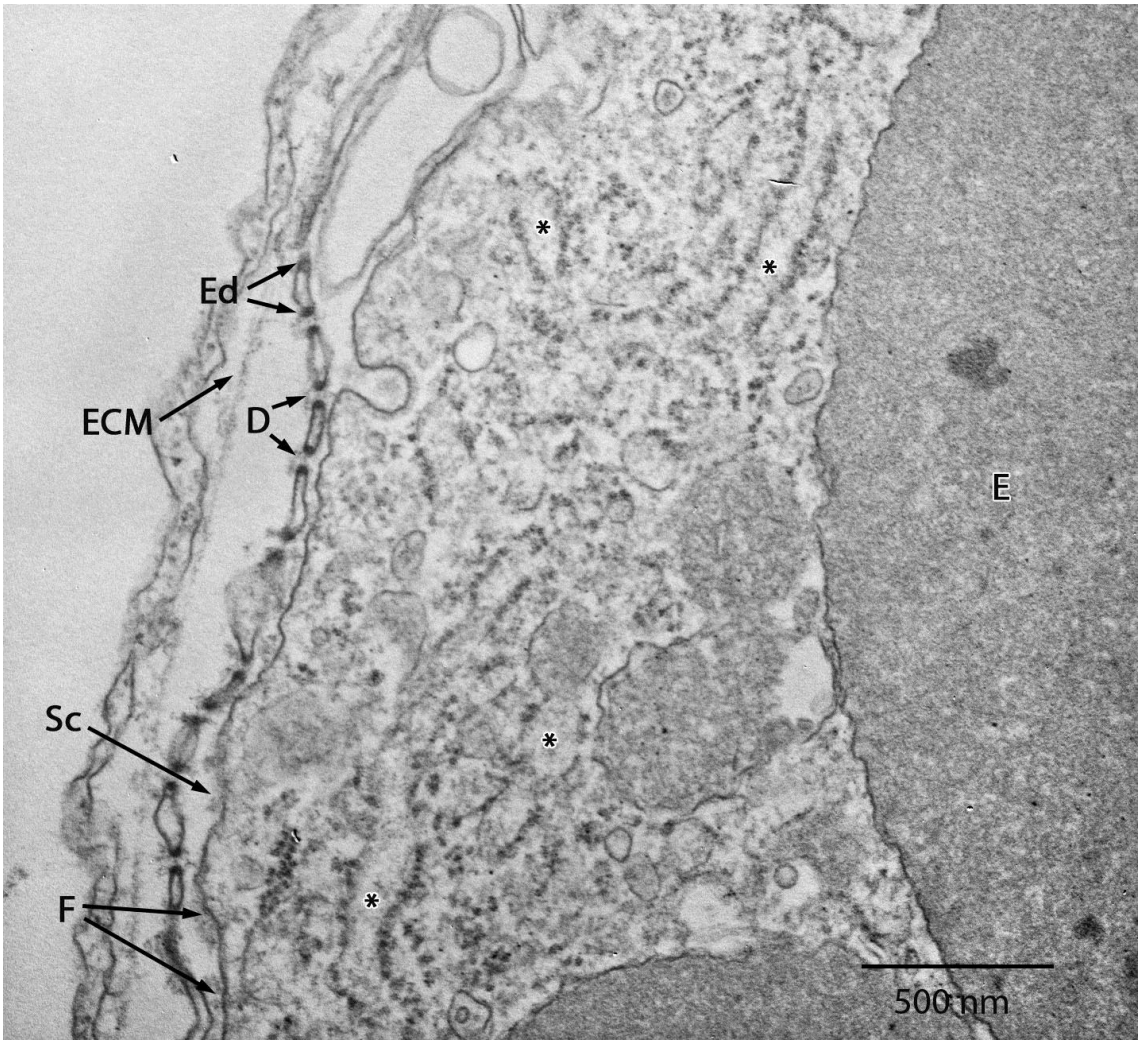

Figure 12. Sieve complex and enlarged RER in a *Marsenina stearnsii* rhogocyte. Characteristic features of a rhogocyte in *Marsenina stearnsii* (TEM, 13 dph). The sieve complex is formed by cytoplasmic bars with regions of increased electron density along their periphery (Ed) underlain by subsurface cisternae (Sc). The slits are spanned by a discontinuous diaphragm (D) and the subsurface cisternae houses floccular material (F) at their base. Regions of the RER are enlarged forming cisternae (*) containing amorphous material. There are also large, moderately electron dense vacuoles (E). Extracellular matrix (ECM).

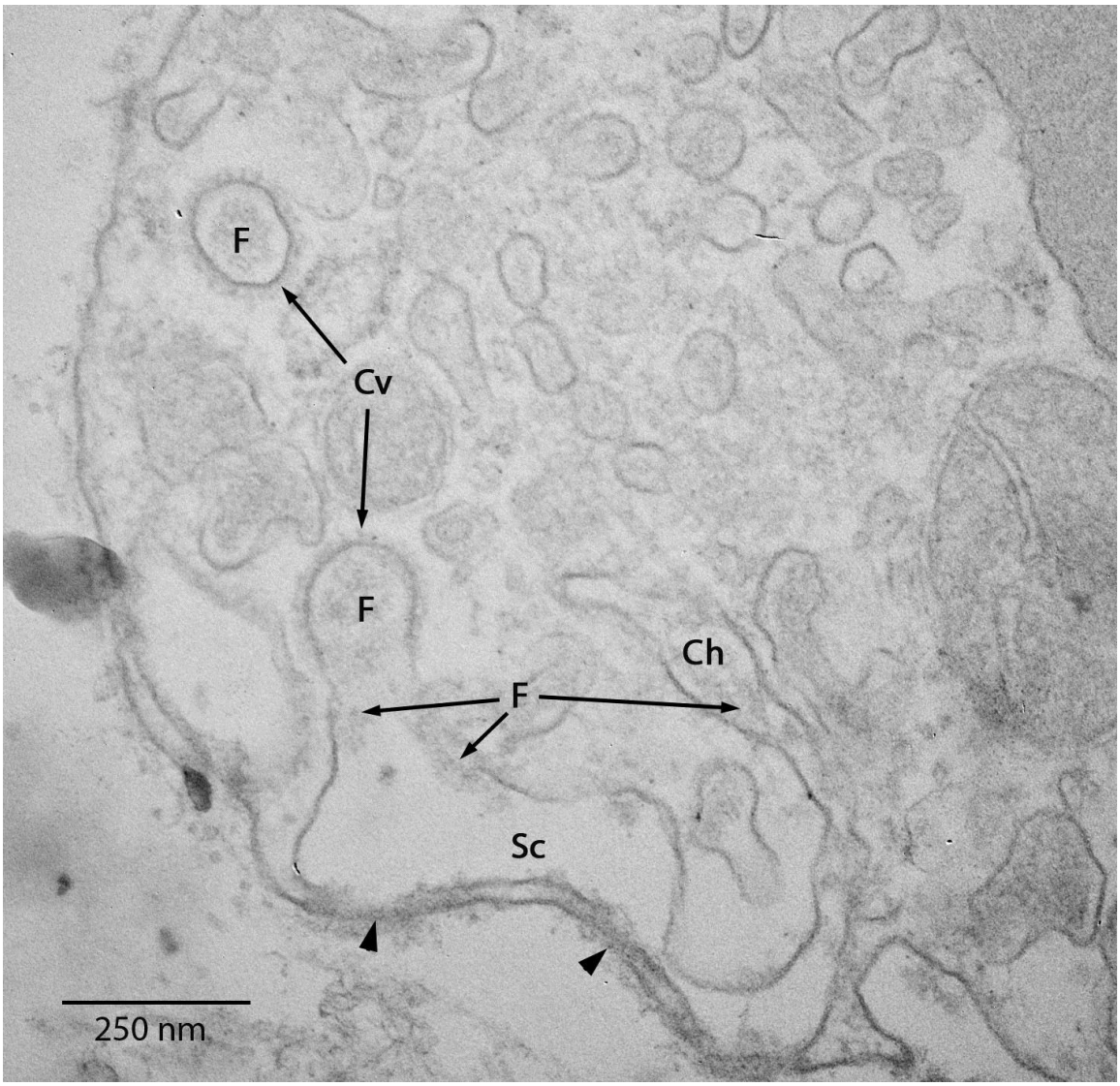

Figure 13. Sieve complex and coated vesicles of a *Marsenina stearnsii* rhogocyte. TEM image of a *Marsenina stearnsii* rhogocyte sieve complex (13 dph). Channels (Ch) extend from the bases of subsurface cisternae (Sc) into the cytoplasm. The coated vesicles (Cv) contain the same floccular material (F) found in the subsurface cisternae and channels. Slits of the sieve complex (arrowheads).

The RER was most notably located at the cell's periphery between the large electron dense vacuoles and the plasma membrane. There was no obvious connection of the RER to the subsurface cisternae, despite their close proximity to each other. There were small regions of RER that were slightly enlarged to a diameter of up to 220 nm and contained amorphous material (Figure 12).

Mitochondria were abundant throughout the entire cell and there were at least two Golgi apparatuses located within each rhogocyte. Large vacuoles containing a medium electron dense material occupied most of the cell volume. In one location, a vacuole appeared to be engulfing up to 12 electron lucent vesicles (Figure 14).

The rhogocytes of *M. stearnsii* were completely surrounded by a continuous, thin layer of ECM (mean thickness of 51.2 ± 34.4 nm, n = 30). The ECM was directly adjacent to the cell in some locations, but was separated by up to 500 nm in others. Where the ECM was not abutting against the plasma membrane, the space between the cell and the ECM was electron lucent (Figure 12).

3.3 Ultrastructure of *Trichotropis cancellata* rhogocytes

Rhogocytes in larvae of *T. cancellata* fixed at 3 dph and were present on either side of the esophagus, as seen in frontal sections taken at the level of the statocysts (Figure 15). The characteristic sieve complexes and electron dense vacuoles identified these cells as rhogocytes (Figure 16). The cytoplasmic bars of the sieve complexes did not have a uniform width (ranging from approximately 110 nm to 315 nm), as seen in *M. stearnsii*. Although the slits were not evenly spaced, their widths were uniform (16.5

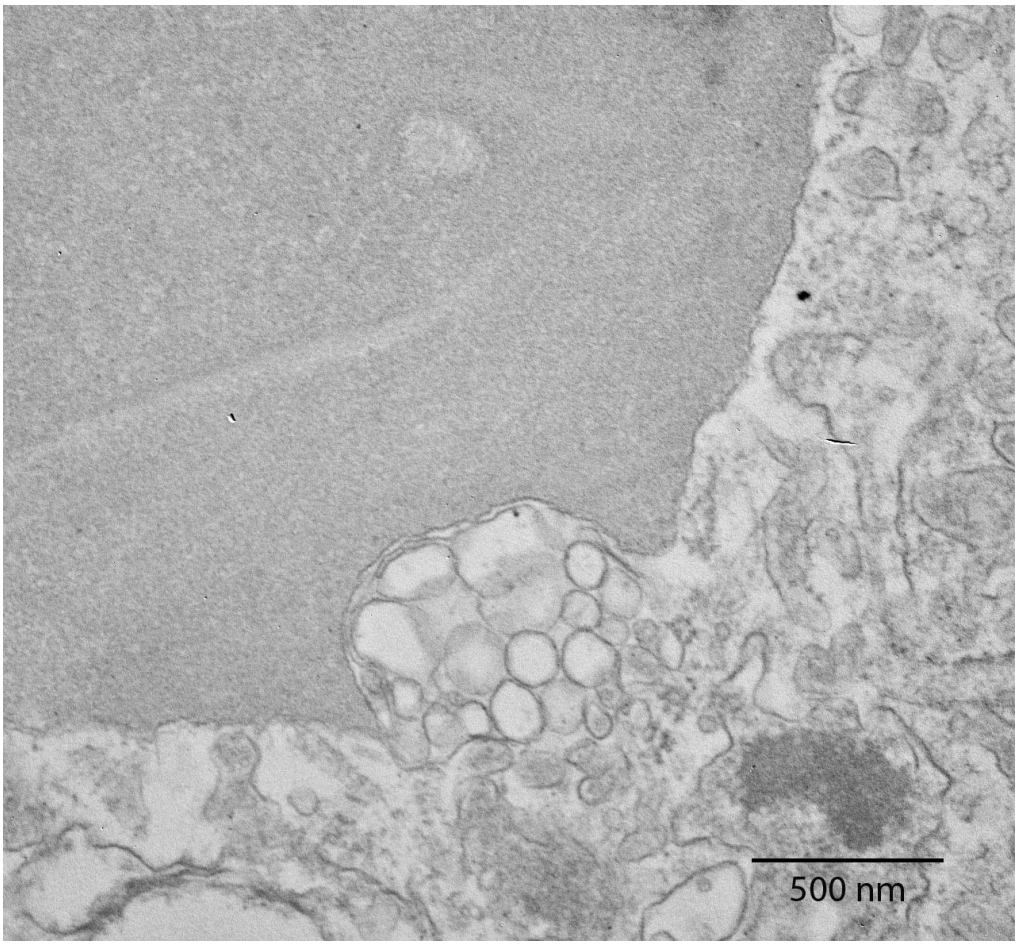

Figure 14. Vacuole of a *Marsenina stearnsii* rhogocyte.

Moderately electron dense vacuole of the rhogocyte of *Marsenina stearnsii* engulfing electron lucent vesicles from the cytoplasm (TEM, 13 dph).

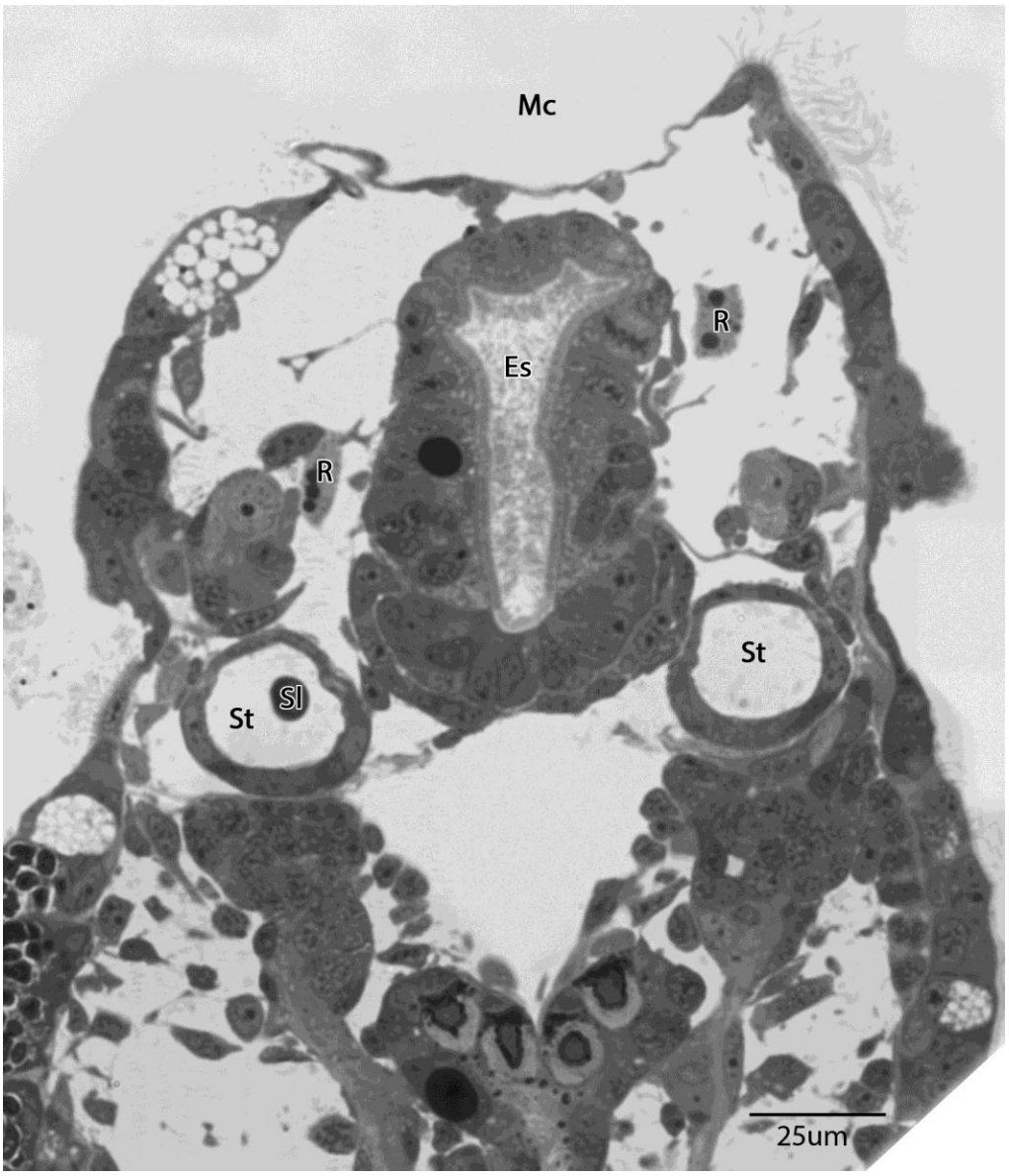

Figure 15. Location of rhogocytes in *Trichotropis cancellata*.

Light micrograph of a *Trichotropis cancellata* larva (frontal section), 3 dph, with a pair of rhogocytes (R) present, one on each side of the esophagus (Es). Mantle cavity (Mc), statolith (Sl), statocyst (St).

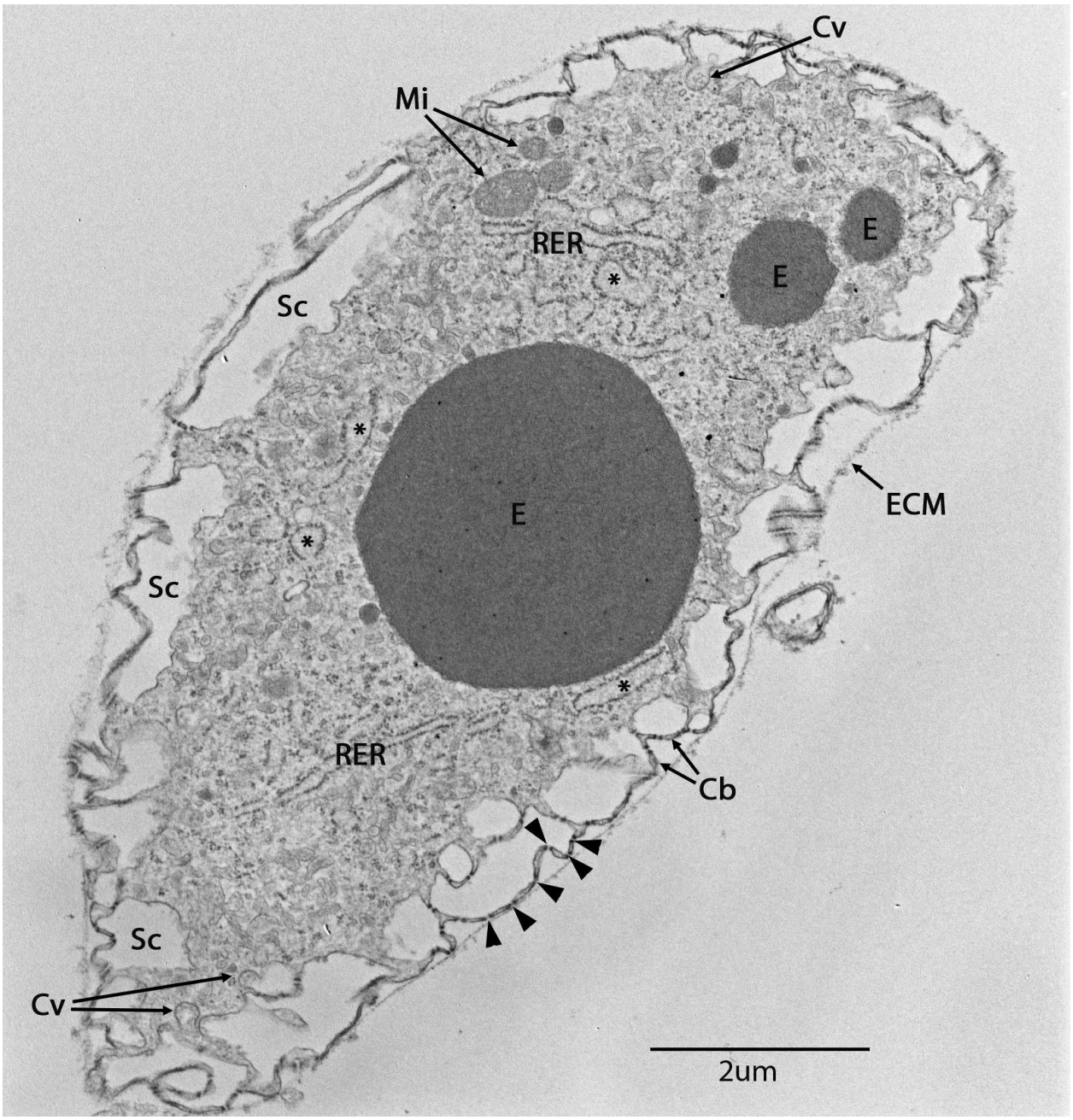

Figure 16. Rhogocyte of *Trichotropis cancellata*.

TEM image of a larval *Trichotropis cancellata* rhogocyte (frontal section, 3 dph). Cytoplasmic bars (Cb) separated by slits (arrowheads), coated vesicles (Cv), moderately electron dense vacuoles (E), extracellular matrix (ECM), mitochondria (Mi), rough endoplasmic reticulum (RER) with enlarged regions filled with amorphous material (*), subsurface cistern (Sc).

± 3.8 nm, n = 25). As in *A. columbiana* and *M. stearnsii* the cytoplasmic bars had a band of increased electron density extending along their lateral margins (Figure 17).

The subsurface cisternae were more narrow than those in *A. columbiana* but deeper than those in *M. stearnsii*. There were numerous occasions where the sieve complexes had a stacked appearance with the slits of the innermost complex open to the cisternae of adjacent complexes (Figure 18). Coated vesicles, continuous with the subsurface cisternae, were present with both stacked and singular sieve complexes. Coated and uncoated vesicles were also present throughout the cytoplasm. These vesicles contained floccular material that was also present in small amounts at the bases of the subsurface cisternae (Figure 17). Multiple uniformly electron dense vacuoles were distributed throughout the cell. In the specimen examined, there were up to seven large vacuoles visible in one section (diameter of at least 0.65 µm) with smaller vacuoles also present.

There were numerous mitochondria of varying sizes throughout the cell. In comparison with the *A. columbiana* and *M. stearnsii* specimens, there was more RER present in the rhogocytes of *T. cancellata*. The RER was densely packed within the cytoplasm and it had regions of enlarged cisternae (diameter up to 330 nm) (Figure 19). Amorphous material was observed within some of these enlarged regions.

The ECM of *T. cancellata* was a fibrous layer (mean thickness of 35.4 ± 14.4 nm, n = 15) surrounding the entire rhogocyte. In some locations the ECM was in contact with the plasma membrane while in other locations it was separated by up to 400 nm. The ECM formed a smooth layer around the irregular shape of the rhogocyte (Figure 18).

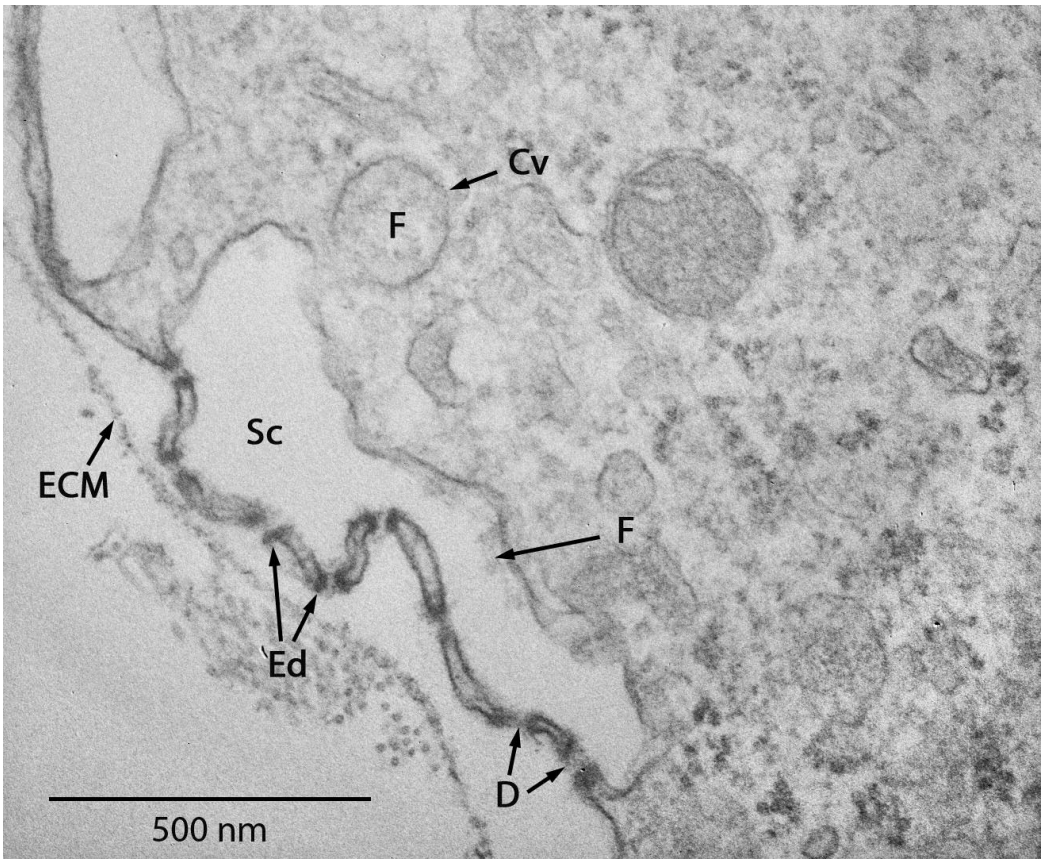

Figure 17. Sieve complex of a *Trichotropis cancellata* rhogocyte.

TEM image of a sieve complex in the rhogocyte of *Trichotropis cancellata* (3 dph) with a coated vesicle (Cv) in close proximity to the base of the subsurface cistern (Sc). The sieve complex consists of a subsurface cistern covered by cytoplasmic bars with regions of increased electron density (Ed) at their edges. The slits between the bars has a discontinuous diaphragm system (D). Floccular material (F) is found within the subsurface cistern and coated vesicle. Extracellular matrix (ECM).

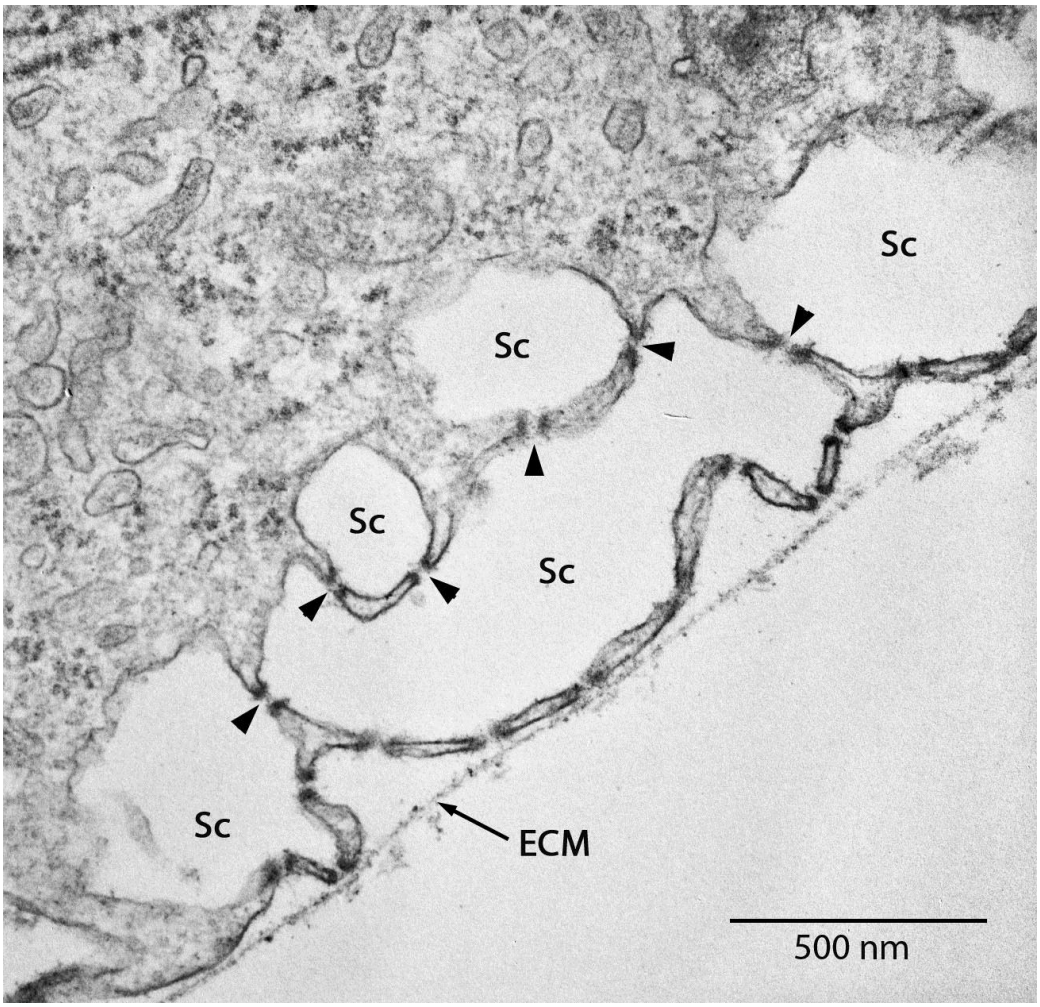

Figure 18. Stacked sieve complexes of a *Trichotropis cancellata* rhogocyte.

Stacked sieve complexes of a *Trichotropis cancellata* rhogocyte (TEM, 3 dph). The slits of the interior-most sieve complexes (arrowheads) open into the subsurface cistern (Sc) of the adjacent sieve complex. Extracellular matrix (ECM).

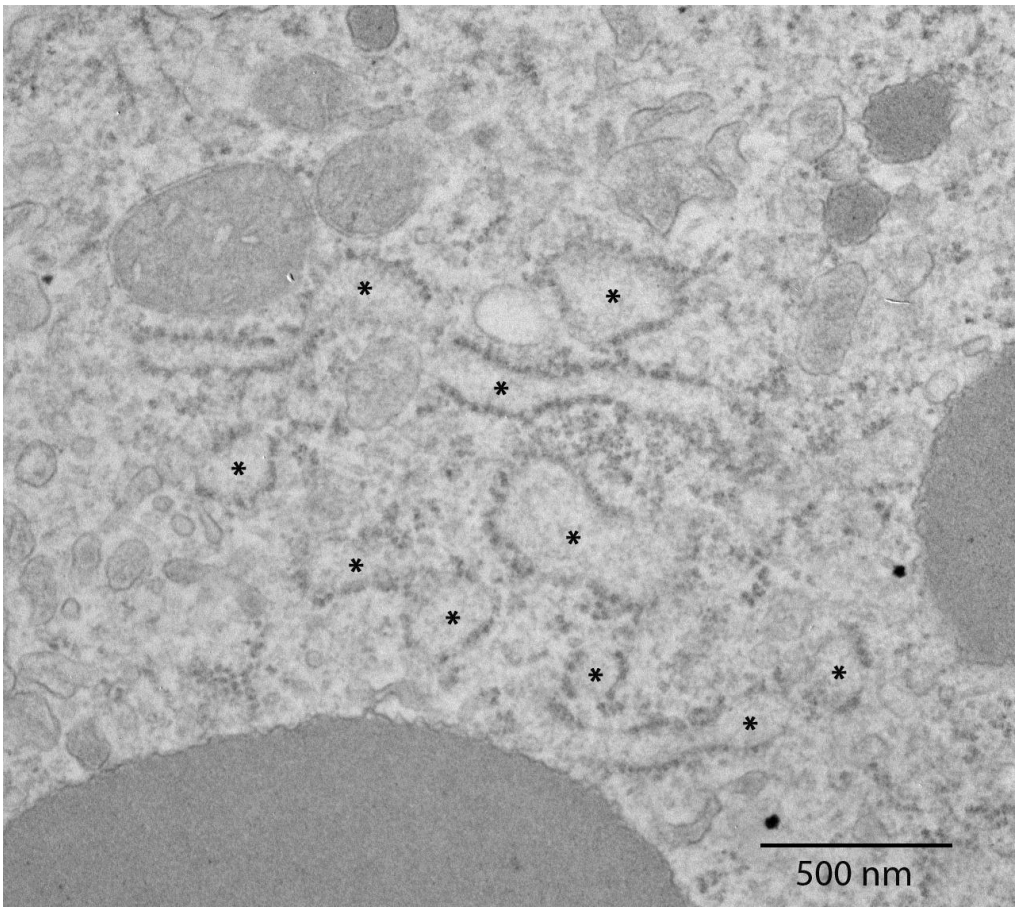

Figure 19. Rough endoplasmic reticulum of a *Trichotropis cancellata* rhogocyte. Enlarged regions of RER (*) within the rhogocyte of *Trichotropis cancellata* (TEM, 3 dph).

3.4 Ultrastructure of *Nerita melanotragus* rhogocytes

Larvae of *N. melanotragus* that were fixed shortly after they were artificially released from the egg capsule had two rhogocytes, one on either side of the distal esophagus (Figure 20). These were identified as rhogocytes by their sieve complexes (Figure 21). The rhogocytes were oval to triangular in shape.

The subsurface cisternae of the rhogocytes of *N. melanotragus* were shallower than those observed in any of the species examined in this study. Furthermore, the subsurface cisternae made up a much smaller proportion of the cellular surface area than in the larval caenogastropods that I examined. The width of the cytoplasmic bars was variable (87.7 ± 23.7 nm, n = 43) and the slit widths also varied, ranging from 17 nm in some locations to 160 nm in others. The cytoplasmic bars, as observed in both cross sections and oblique sections, were joined by diaphragms as described by Boer and Sminia (1976). In cross section these diaphragms were visible as thin layers protruding from the cytoplasmic bars into the slits. At the periphery of each cytoplasmic bar was a small region of increased electron density as was seen in all other species examined (Figure 22).

There were coated vesicles continuous with the narrow subsurface cisternae (Figure 22) as well as free in the cytoplasm (Figure 23). These vesicles as well as the subsurface cisternae contained floccular material. There were some sieve complexes in the plasma membrane that appeared to be stacked like those observed in *A. columbiana* and *T. cancellata* (Figure 24).

Figure 20. Location of rhogocytes in *Nerita melanotragus*.

Light micrograph of a frontal section of *Nerita melanotragus* larva immediately after release from the egg capsule. Rhogocytes (R) are located to either side of the distal esophagus (Es).

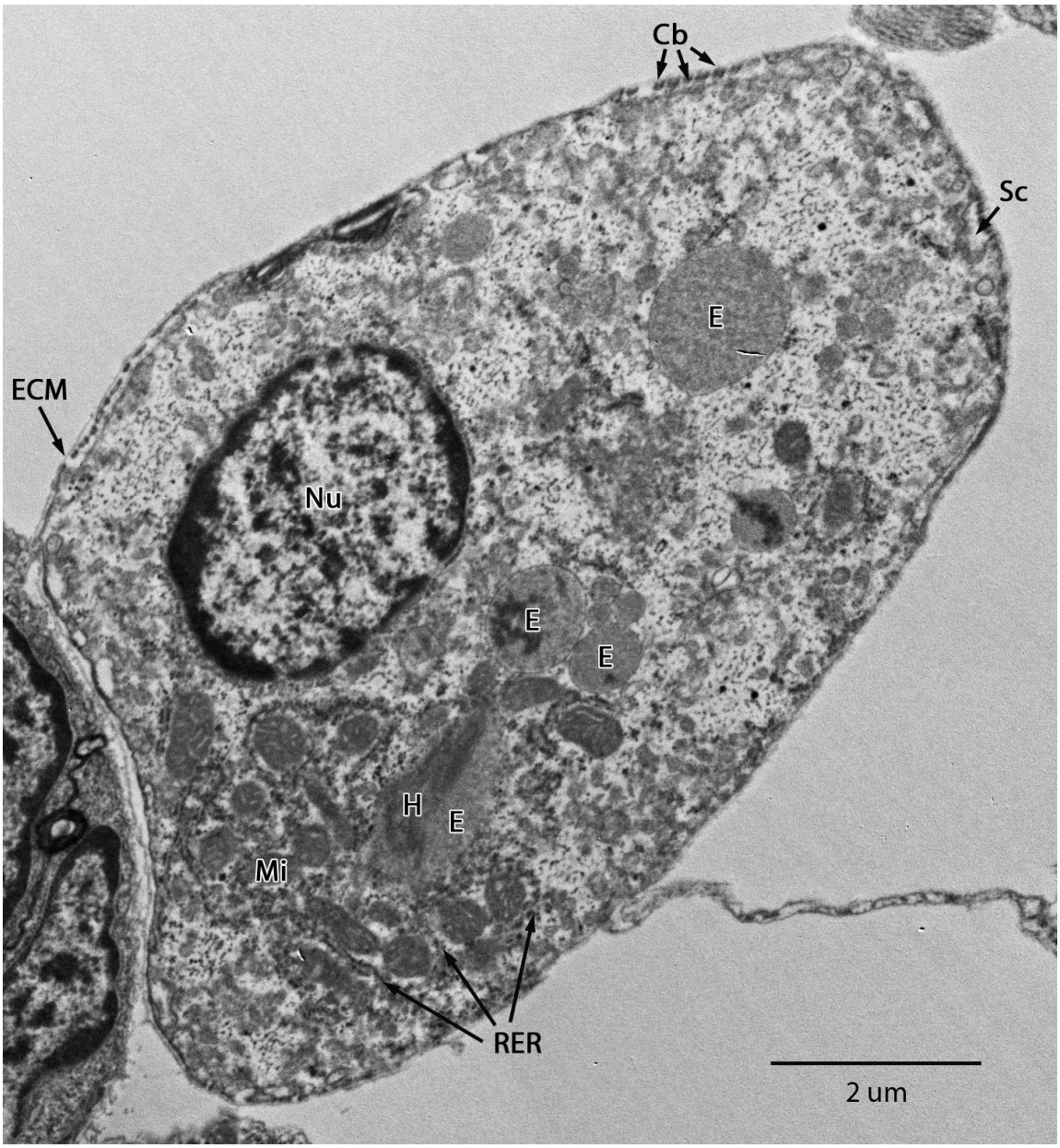

Figure 21. *Nerita melanotragus* rhogocyte.

TEM image of a rhogocyte in a larval *Nerita melanotragus* (frontal section, immediately after hatching). Hemocyanin molecules (H) were visible in a moderately electron dense vacuole (E). Cytoplasmic bars (Cb), extracellular matrix (ECM), mitochondria (Mi), nucleus (Nu), rough endoplasmic reticulum (RER), subsurface cisterna (Sc).

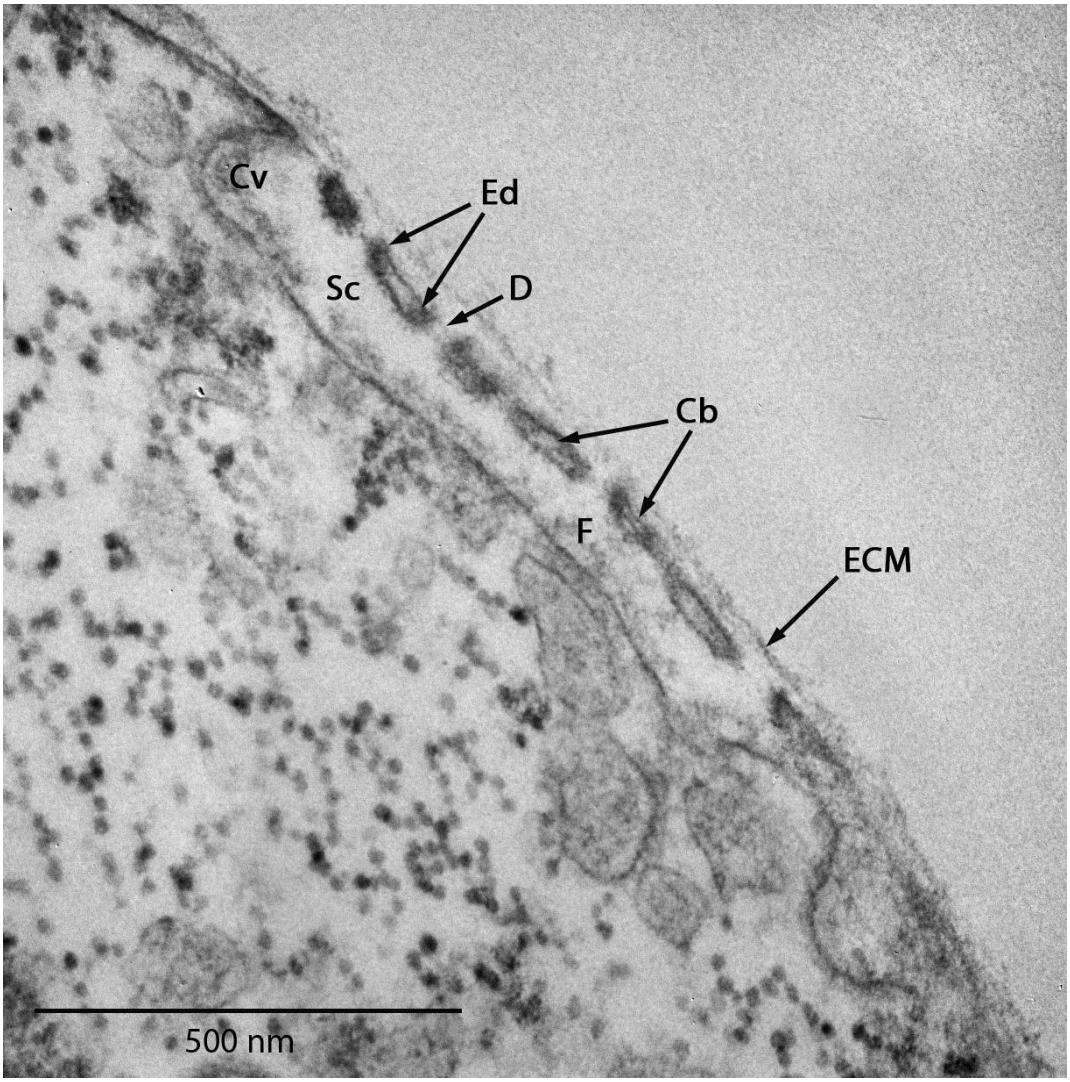

Figure 22. Sieve complex of a rhogocyte in *Nerita melanotragus*.

A sieve complex of a *Nerita melanotragus* rhogocyte (TEM, immediately after hatching). The sieve complex is composed of cytoplasmic bars with electron dense lateral margins (Ed) with slits spanned by thin diaphragms (D) between them. There is a coated vesicle (Cv) continuous with the subsurface cisterna (Sc), both containing floccular material (F). The sieve complex is overlain by an extracellular matrix (ECM).

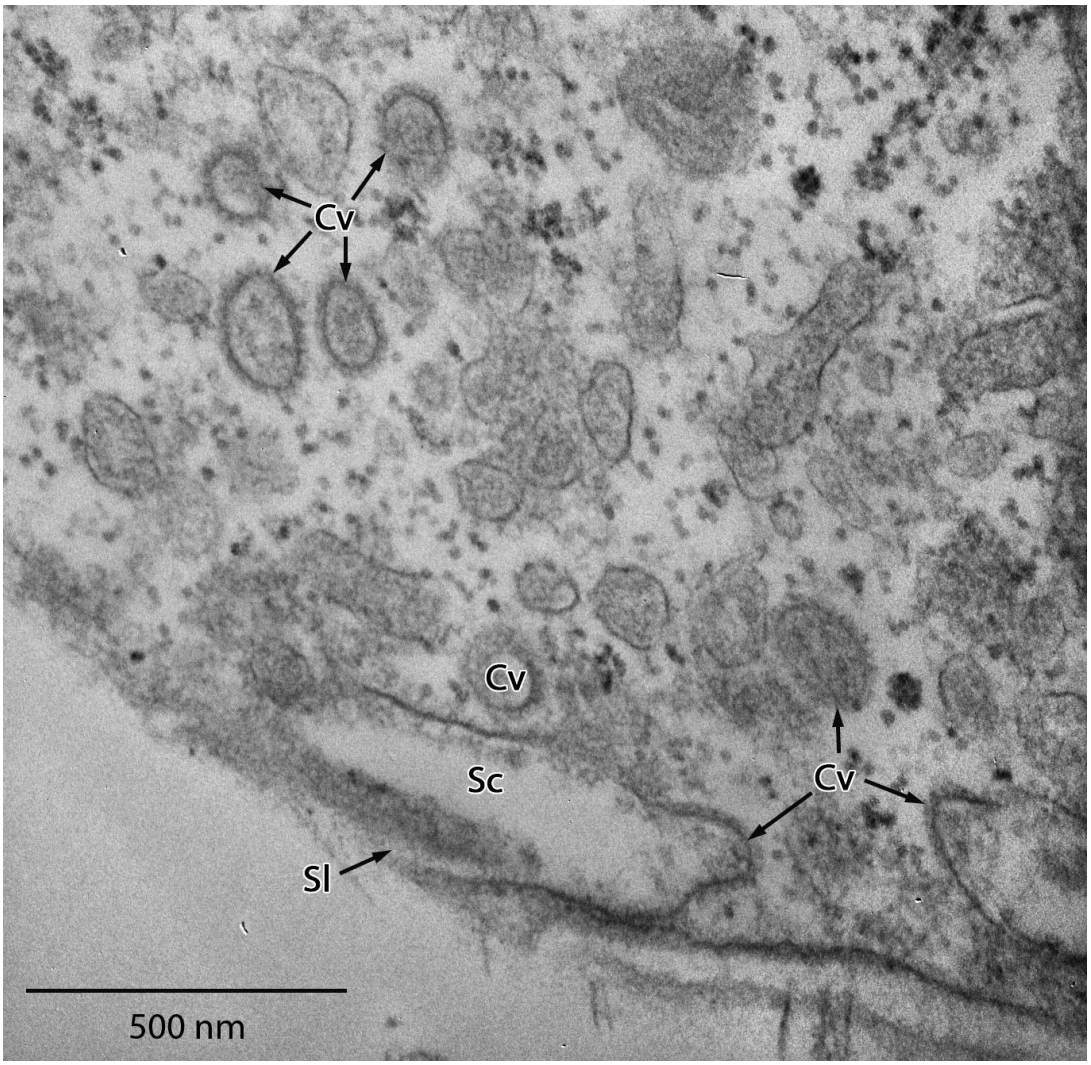

Figure 23. Coated vesicles in a *Nerita melanotragus* rhogocyte.

TEM image showing coated vesicles (Cv) in a larval *Nerita melanotragus* rhogocyte (immediately after hatching). The vesicles are found continuous with the subsurface cisterna (Sc) and free in the cytoplasm, both containing floccular material. Slit of a sieve complex (Sl).

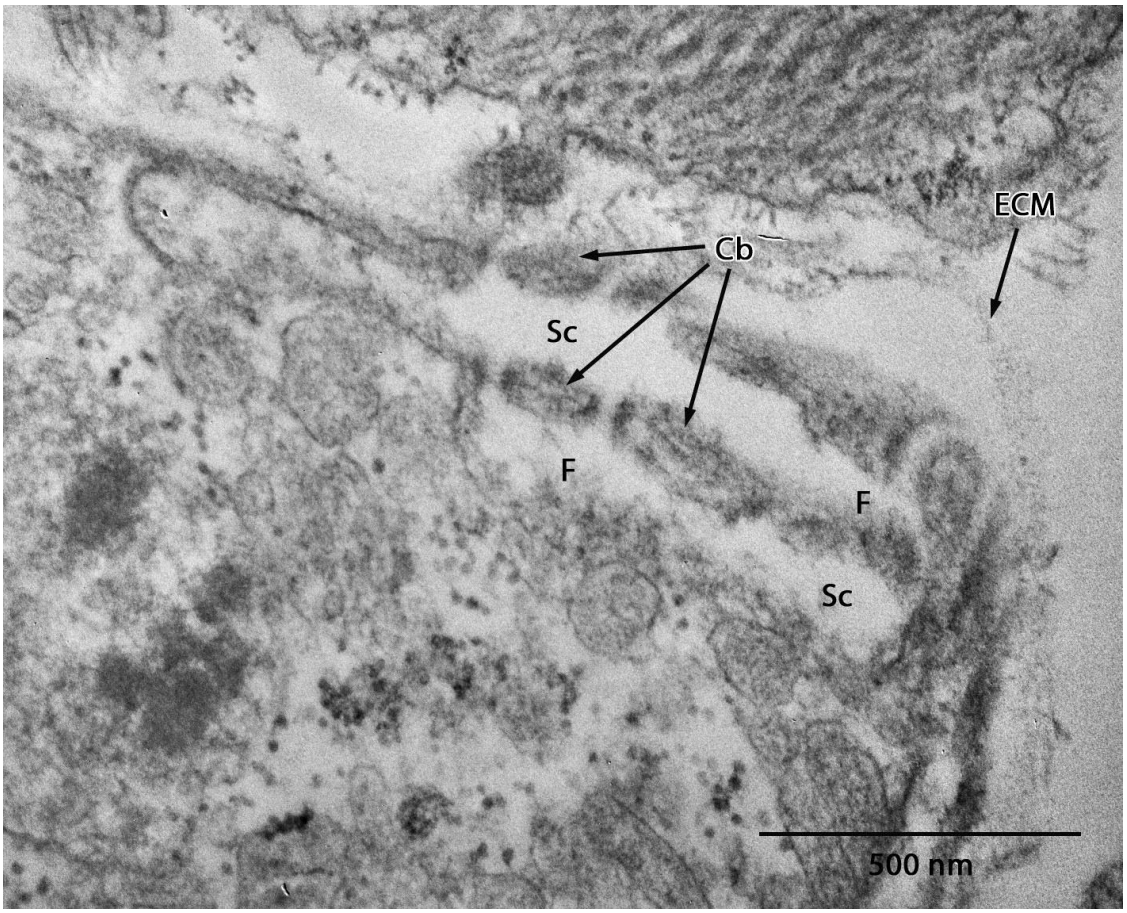

Figure 24. Stacked subsurface cisternae in a *Nerita melanotragus* rhogocyte. Stacked subsurface cisternae (Sc) of a rhogocyte of *Nerita melanotragus* (TEM, immediately after hatching). Cytoplasmic bars (Cb), extracellular matrix (ECM) and floccular material (F).

The larval rhogocytes in *N. melanotragus* had a prominent round nucleus. There were many mitochondria with the majority concentrated at one end of the cell. These mitochondria were surrounded by dense RER (Figure 25).

The *N. melanotragus* rhogocytes also contained the characteristic large vacuoles of rhogocytes observed in other larval gastropods. Some of the vacuoles were uniformly electron dense, while others contained regions of much higher electron density. Within the largest vacuole of each rhogocyte were bundles of long, hollow rods that appeared to be hemocyanin molecules (Figure 26). These rods were tightly packed into bundles within the vacuoles. These were identified as HCN molecules based on their structural characteristics. The rods had a hollow, cylindrical structure with a diameter of 35.1 nm ± 1.2 nm (n = 5) (Figure 27).

The extracellular matrix surrounding the rhogocyte had a fibrous appearance. The ECM was directly adjacent to the plasma membrane of the cell with the maximum distance between the ECM and the cell being 165 nm.

3.5 Ultrastructure of *Siphonaria denticulata* cyrtocytes

Larvae of *S. denticulata* were fixed immediately after hatching. In frontal sections, cyrtocytes of the protonephridia were observed on each side of the esophagus, dorsal to the cerebral ganglia (Figure 28).

The morphology of the cyrtocytes of larval *S. denticulata* was consistent with that of cyrtocytes described by Smith and Ruppert (1988; Ruppert and Smith, 1988; Smith,

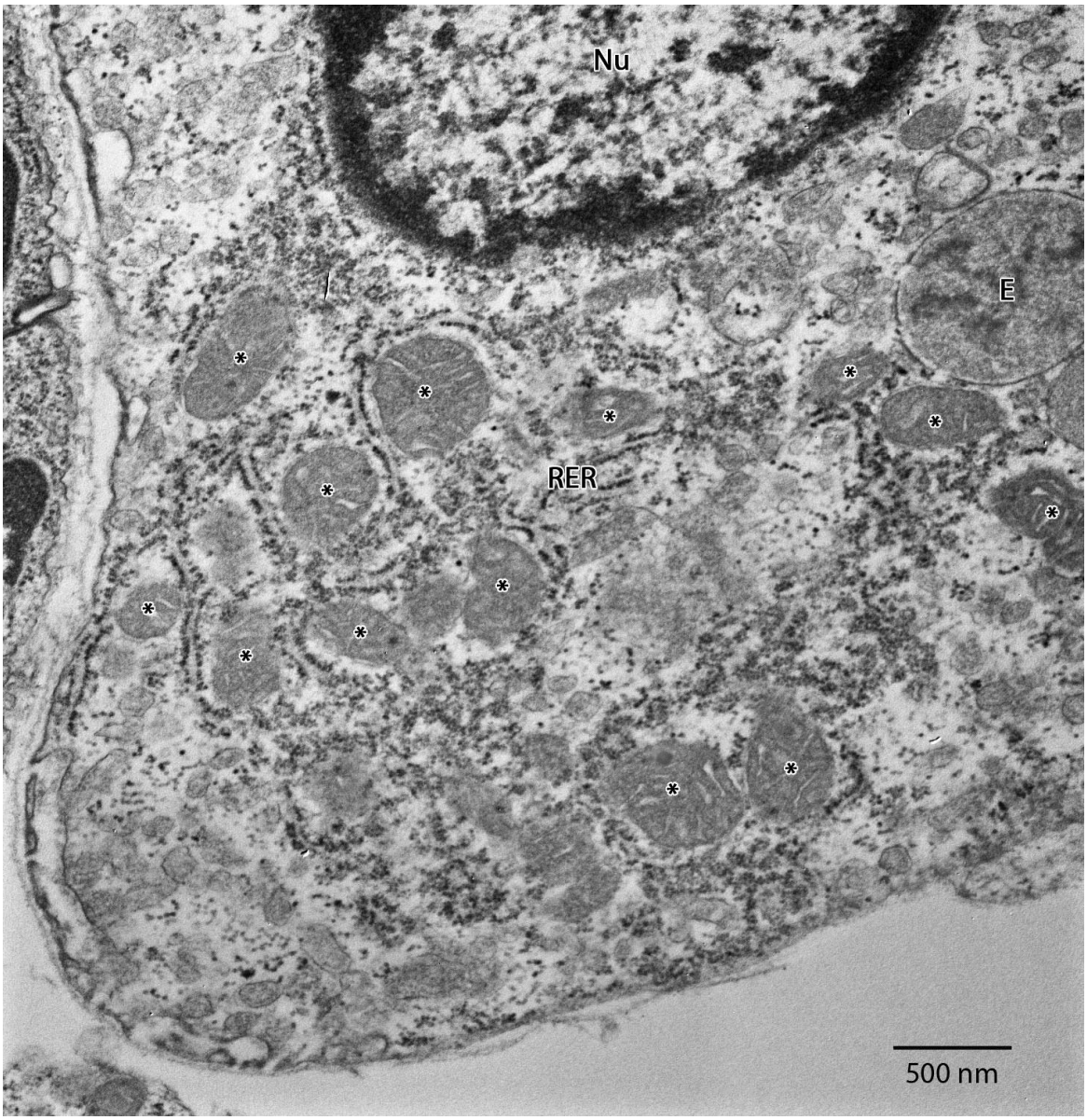

Figure 25. Rough endoplasmic reticulum in a *Nerita melanotragus* rhogocyte.
TEM image of a *Nerita melanotragus* rhogocyte immediately after hatching showing densely packed rough endoplasmic reticulum (RER) surrounding multiple mitochondria (*). Moderately electron dense vacuole (E), nucleus (Nu).

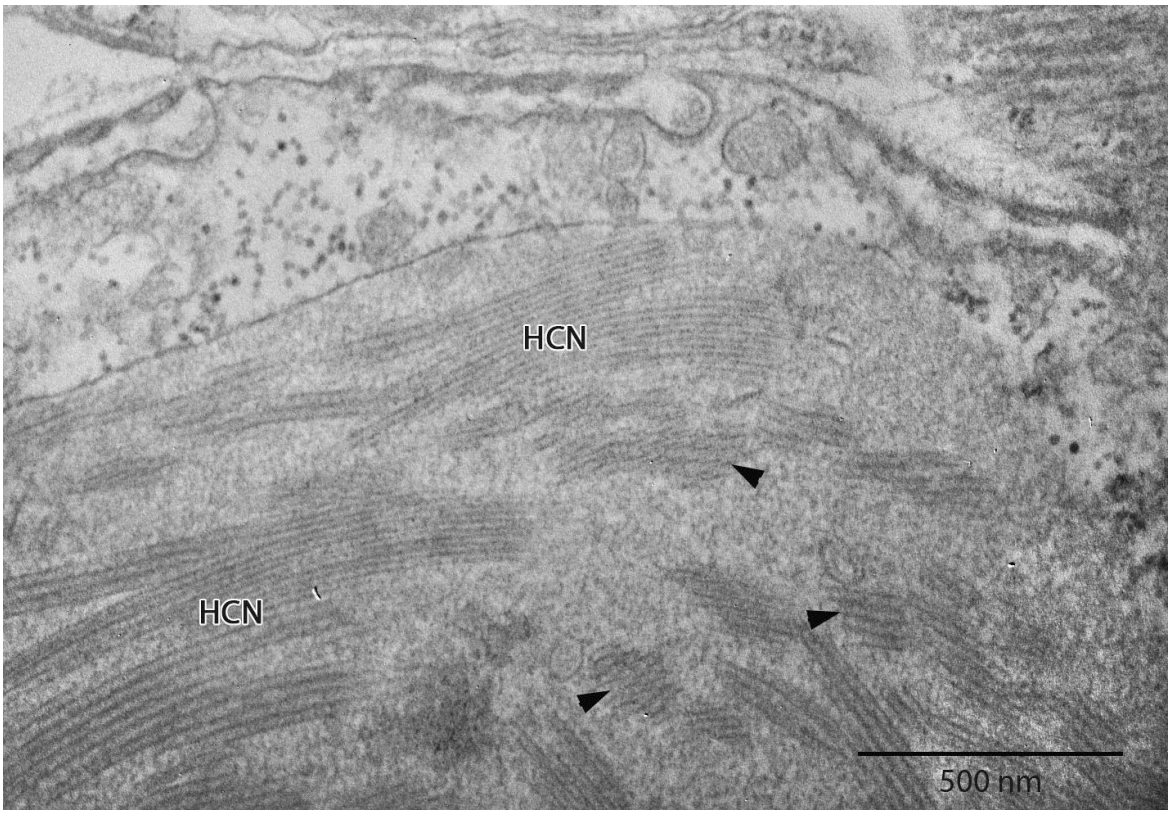

Figure 26. Vacuole containing hemocyanin in a *Nerita melanotragus* rhogocyte.
A moderately electron dense vacuole in a rhogocyte of *Nerita melanotragus* (TEM, immediately after hatching) containing hemocyanin molecules (HCN). The hemocyanin molecules form bundles of long rods which in cross section have a circular appearance (arrowheads).

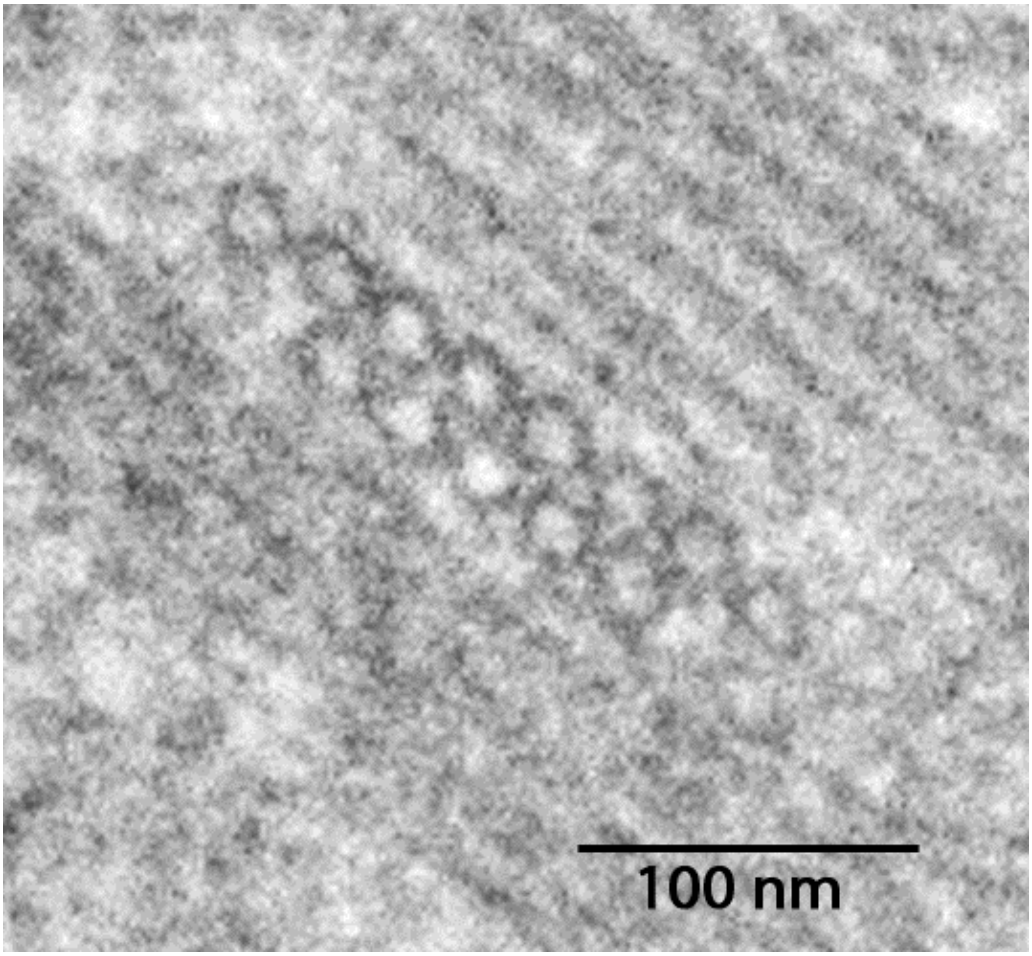

Figure 27. Hemocyanin molecules in a *Nerita melanotragus* rhogocyte.

Cross section of hemocyanin molecules within a vacuole of a *Nerita melanotragus* rhogocyte (TEM, immediately after hatching).

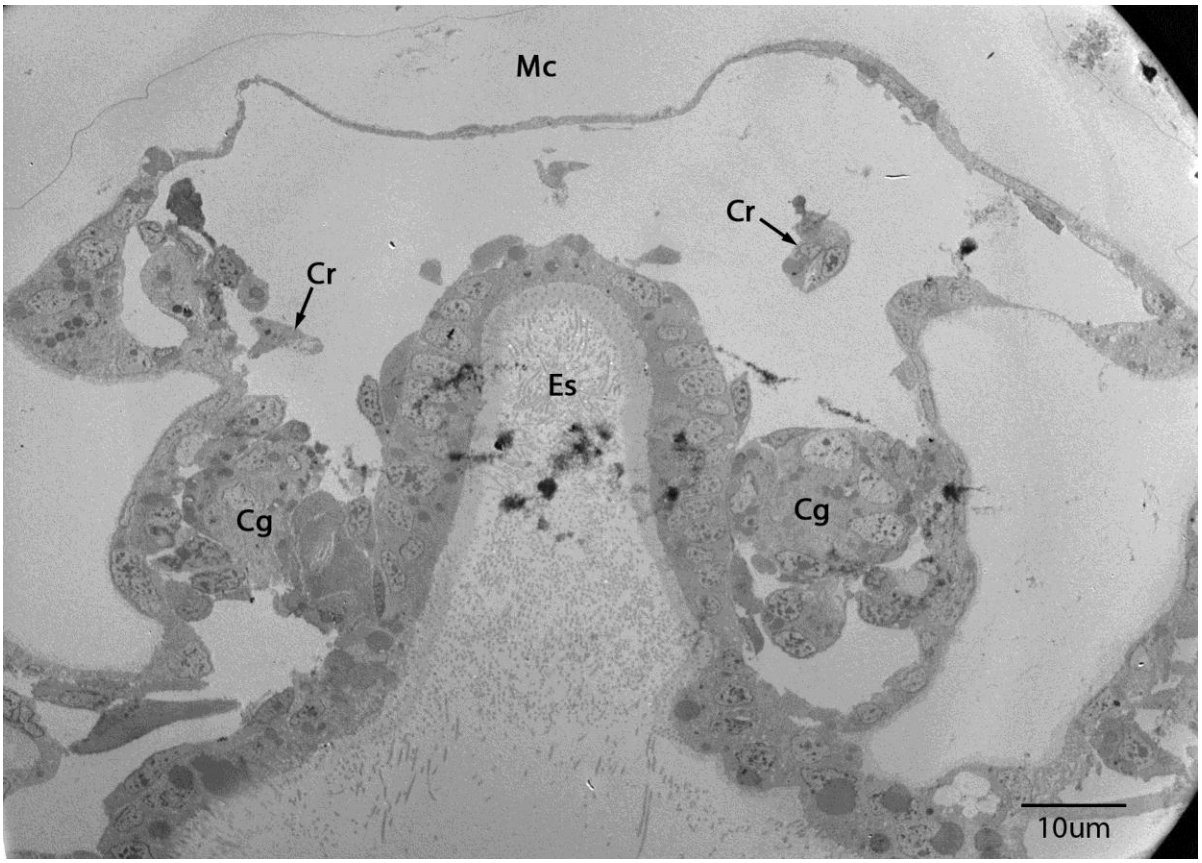

Figure 28. Location of cyrtocytes in *Siphonaria denticulata.*

Frontal section of *Siphonaria denticulata* immediately after hatching (TEM). Cyrtocytes (Cr), cerebral ganglia (Cg), esophagus (Es), mantle cavity (Mc).

1992; Ruppert, 1994). The cyrtocytes were multiciliated with extensions of the cell body forming a collar surrounding the cilia (Figure 29). The extensions had a sieve-like structure for filtration that was created by a system of cytoplasmic bars separated by narrow slits, spanned by a thin diaphragm (Figure 30). The edges of the cytoplasmic bars, adjacent to the slit opening, exhibited a region of increased electron density that did not extend into the middle of the bar. These cytoplasmic bars had different widths and they created inconsistent spacing between the slits of the sieve structure. The cell was surrounded basally by a thin ECM of fibrous and floccular material.

The majority of the cyrtocyte cell body was occupied by a large, irregularly shaped nucleus (Figure 29). Within the cell body were also numerous large mitochondria and electron dense vacuoles. Some of these vacuoles were uniformly electron dense whereas others had variable electron densities. There were coated and uncoated vesicles present within the cytoplasm of the cyrtocyte. Coated vesicles that were observed attached to the plasma membrane were located in regions away from the sieve structures (Figure 31).

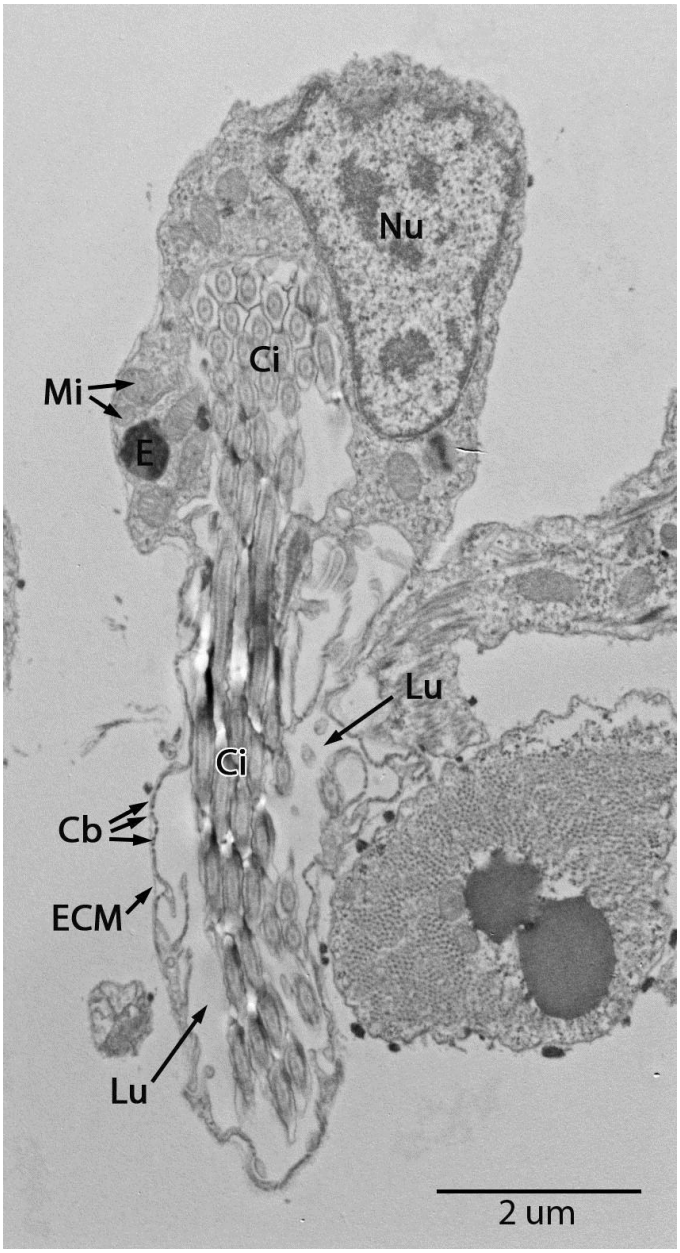

Figure 29. *Siphonaria denticulata* cyrtocyte.

TEM image of a cyrtocyte of *Siphonaria denticulata* immediately after hatching. Cytoplasmic bars (Cb), cilia (Ci), electron dense vacuole (E), extracellular matrix (ECM), lumen (Lu), mitochondria (Mi), nucleus (Nu).

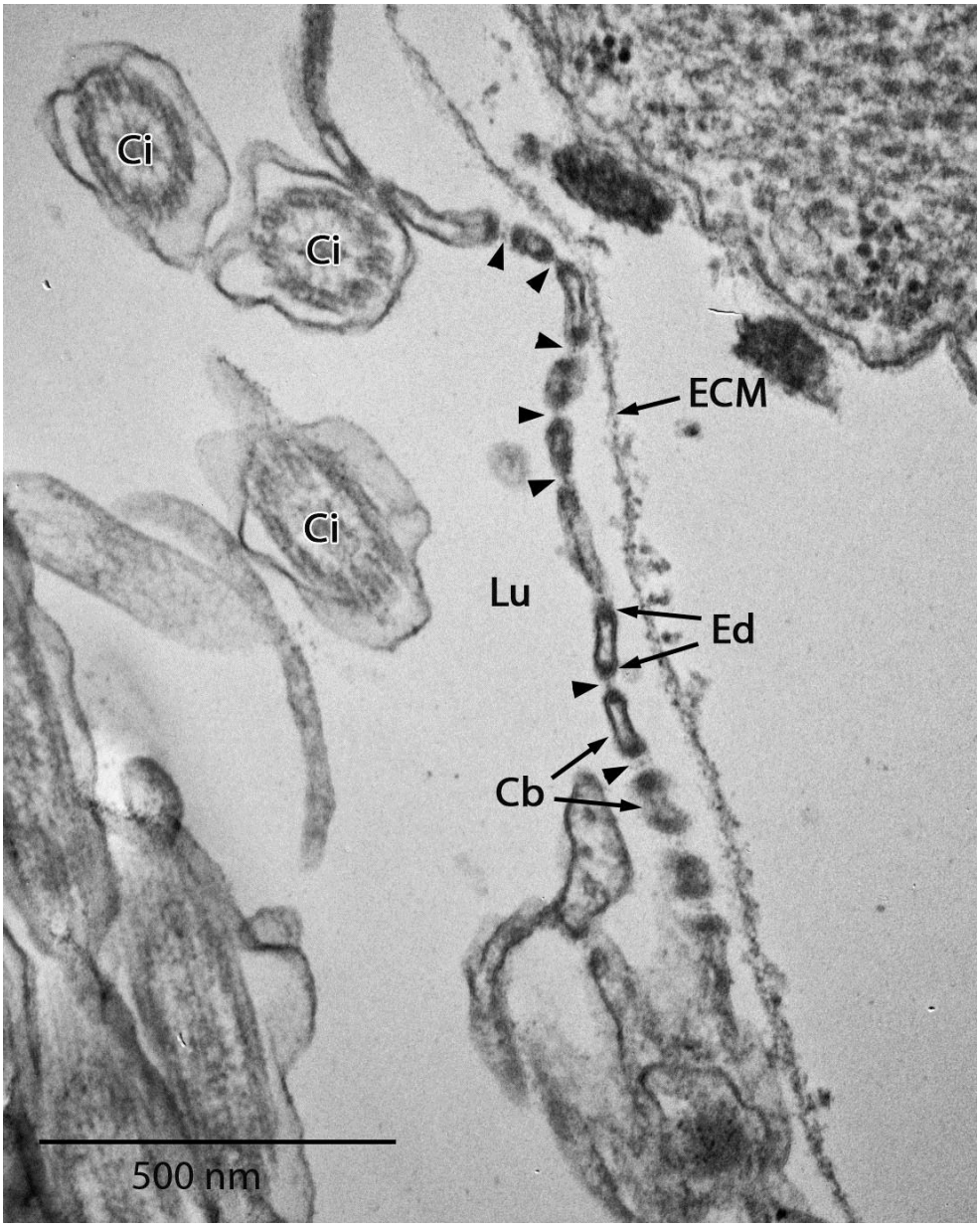

Figure 30. Location of filtration in a *Siphonaria denticulata* cyrtocyte.

Site of filtration in a cyrtocyte of *Siphonaria denticulata* (TEM, immediately after hatching). Filtration occurs across the cytoplasmic bars (Cb) with electron dense regions on their periphery (Ed) into the lumen of the cyrtocyte (Lu) and is aided by the extracellular matrix (ECM). The openings between the cytoplasmic bars (arrowheads) have thin, discontinuous diaphragms. Cilia (Ci) create negative pressure drawing fluid across the site of filtration.

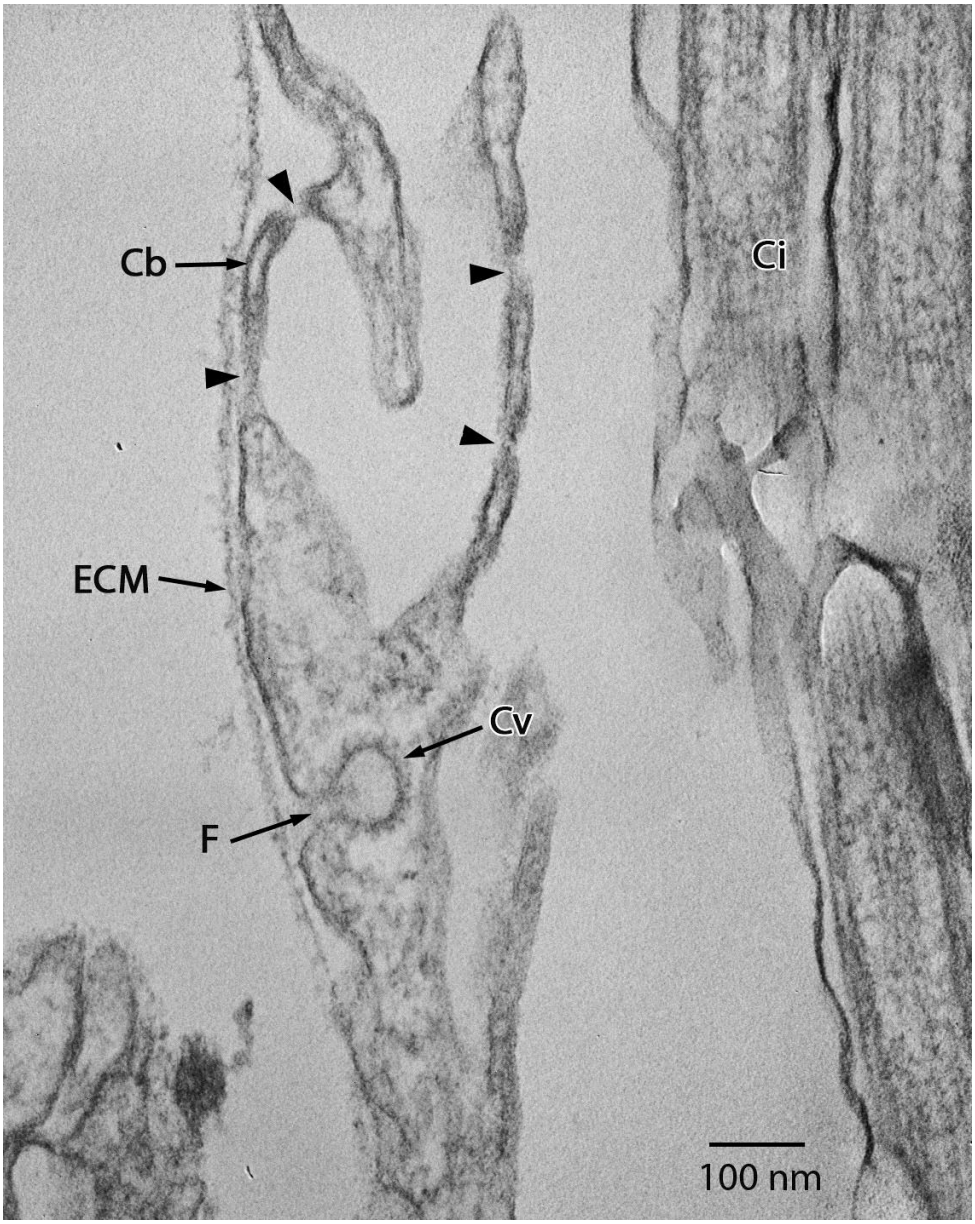

Figure 31. Coated vesicle and sieve structure of a *Siphonaria denticulata* cyrtocyte. Coated vesicle (Cv) fused with the plasma membrane of a cyrtocyte in *Siphonaria denticulata* (TEM, immediately after hatching) in a region away from the site of filtration, the cytoplasmic bars (Cb) and slits between them (arrowheads). There is floccular material (F) in the neck of the coated vesicle. Cilia (Ci), extracellular matrix (ECM).

4.0 Discussion

The distinctive molluscan cell type known as a rhogocyte has been extensively documented in adult molluscs (reviewed by Haszprunar, 1996; Albrecht *et al.*, 2001; Martin *et al.*, 2011) and in non-feeding developmental stages of a direct developing gastropod (Fioroni *et al.*, 1984). The observations presented here are the first to identify rhogocytes in planktotrophic (feeding) larvae of any mollusc. My ultrastructural survey of larvae from three major groups of gastropods identified rhogocytes in three species of caenogastropods and a species of neritimorph, but did not identify these cells in a larval heterobranch. These results fill a major gap as Gastropoda is the largest class of Mollusca and the majority of gastropods have a life history that includes a pelagic larval stage that must feed to achieve metamorphic competence. The discovery of rhogocytes in long-lived, feeding larvae of at least some species of gastropods may help to identify the possible multiple functions of this molluscan cell type.

Rhogocytes in larvae were identified by sieve complexes formed by their plasma membrane underlain by subsurface cisternae and moderately electron dense vacuoles in the cytoplasm. These ultrastructural characteristics are consistent with rhogocytes described in connective tissue structures of adult gastropods, such as the pulmonates (Heterobranchia) *Lymnaea stagnalis* (Sminia *et al.*, 1972; Sminia and Boer, 1973), *Achatina achatina* (Skelding and Newell, 1975) and *Helix aspersa* (Smina and Vlugt-van Daalen, 1977) and the vetigastropods *Haliotis tuberculata* (Albrecht *et al.*, 2001) and *Megathura crenulata* (Martin *et al.*, 2011). Furthermore, rhogocytes identified in post-hatching planktotrophic larvae of three species of caenogastropod and one species of

neritimorph were found in the same location as those described in embryos of the direct developing caenogastropod *Nucella lapillus* (Fioroni *et al*., 1984).

Despite the global similarities in rhogocytes described from adult and larval gastropods, I also identified some differences. The presence of stacked sieve complexes has not been previously documented in rhogocytes. Stacked sieve complexes were observed in rhogocytes of both *A. columbiana* and *T. cancellata*. The function of these stacked complexes is unknown. Rhogocytes have been shown to selectively take up substances based on size (for example, Sminia, 1972; Skelding and Newell, 1975; Boer and Sminia, 1976); therefore it is possible that having stacked sieve complexes could increase selectivity. However, since the slits in each tier of sieve complex were the same width, increasing selectivity based on size is unlikely. A second potential difference between larval and adult rhogocytes in gastropods relates to the presence of coated vesicles associated with the subsurface cisternae. These were abundant in larval rhogocytes of the species that I examined, but Haszprunar's (1996) review of rhogocyte structure in adult molluscs suggests that vesicles are rarely associated with subsurface cisternae. However, this aspect of rhogocyte structure is controversial because Prince and Johnson (2006) observed numerous coated vesicles associated with the subsurface cisternae of rhogocyte-like cells within the ink gland of adult *Aplysia californica*.

4.1 Possible functions of rhogocytes in gastropod larvae

The function of molluscan rhogocytes is controversial. Although many functions have been suggested, evidence for some of these functions remains weak. The function

that has received the best-documented support from both ultrastructural and molecular evidence is synthesis of hemocyanin in adult vetigastropods (Albrecht *et al.*, 2001; Martin *et al.*, 2011). Nevertheless, strong evidence for hemocyanin synthesis by rhogocytes is not apparent for all species of molluscs; for example, Haszprunar's (1996) review of rhogocyte ultrastructure states that evidence of HCN in rhogocytes is rare. Results of other studies have suggested that rhogocytes may be involved in the concentration and detoxification of heavy metals (Marigómez *et al.*, 2002), or may sequester damaged HCN for degradation (Beuerlein *et al.*, 2002b). Prince and Johnson (2006) have even suggested that rhogocytes are involved in the synthesis and transport of ink within the ink gland of aplysiids.

The function of rhogocytes in larval gastropods is similarly enigmatic. My comparative analysis of rhogocytes in a diversity of larval gastropods, when combined with previous research on this cell type and biological knowledge about the larval species studied, may begin to open a window of understanding into the role of these cells in gastropod larvae. Ultrastructural observations on rhogocytes from larvae of three species of caenogastropods revealed no evidence of HCN within the rhogocytes, whereas vacuoles within newly released larvae of *N. melanotragus* were packed with apparent HCN didecamers. I explore a possible explanation for this discrepancy, however this and other explanations need to undergo further testing in future studies.

Although rhogocytes in the larval caenogastropods *A. columbiana*, *M. stearnsii* and *T. cancellata* contained no discernible HCN molecules within any subcellular compartment, they nevertheless appeared to be undergoing active protein synthesis as indicated by the abundant RER and Golgi complexes. Rhogocytes in these larvae also

showed numerous coated and uncoated vesicles associated with the subsurface cisternae. The substances these vesicles are transporting and the direction of movement are unknown. In contrast, rhogocytes in the neritimorph, *N. melanotragus*, contained vacuoles that were packed with apparent HCN molecules, which have been described as hollow cylinders having a diameter of approximately 35 nm (Bonaventura and Bonaventura, 1980; Ryan *et al.*, 1985; Albrecht *et al.*, 2001, Manubens *et al.*, 2010). The cylinders of HCN were arranged linearly, similar to the arrangement described by Albrecht *et al.* (2001) in *H. tuberculata*. Furthermore, larvae of *N. melanotragus* showed few profiles of RER and few coated vesicles associated with the subsurface cisternae beneath sieve complexes.

A possible explanation for the abundance of HCN molecules within larval rhogocytes of *N. melanotragus*, but an apparent lack of HCN molecules within larval rhogocytes of three species of caenogastropods may relate to evidence of a pre-hatching diapause in *N. melanotragus*. Observations of several species within the genus *Nerita* suggest that encapsulated embryos of at least some members of this genus may be incapable of hatching when egg capsules are continuously submerged (Risbec, 1932; Anderson, 1962; L.R. Page, unpublished observations). These inhabitants of the high intertidal zone may delay hatching until appropriate environmental conditions occur, which are not replicated within laboratory aquaria (Risbec, 1932; Anderson, 1962). More surprisingly, both Risbec (1932) and Page (L.R. Page, unpublished observations) found evidence that encapsulated embryos of *N. albicilla* and *N. melanotragus* may enter a state of developmental arrest during a delay of hatching interval that may last for 1-2 months or longer. When egg capsules of *N. melanotragus* were artificially opened during this

delay of hatching period, the fully formed larvae inside were totally inert, but they began to actively swim between 0.5 to 3 min (L.R. Page, unpublished observations). The larvae of *N. melanotragus* that I examined were fixed within 6 hours after they were artificially released from their egg capsules. Prior to the onset of pre-hatching diapause, rhogocytes within embryos of this species may have synthesized HCN which was subsequently stored within intracellular vacuoles during the diapause interval. Arrest of synthetic activity during diapause would explain the absence of RER profiles within rhogocytes of *N. melanotragus* that were examined soon after their release from their egg capsules. Caenogastropod larvae may also synthesize HCN, but these molecules may be exported immediately to the hemal fluid so that HCN does not accumulate within rhogocytes.

The hypothesis that HCN in *N. melanotragus* embryos is stored after synthesis, rather than continuously exported, is consistent with the location of HCN molecules within intracellular vacuoles in larvae fixed shortly after their release from an intracapsular diapause. When HCN molecules have been resolved within rhogocytes of adult gastropods, they occur within the RER or the subsurface cisternae (Sminia and Boer, 1973; Skelding and Newell, 1975; Albrecht *et al.*, 2001; Martin *et al.*, 2011). Rhogocytes within post-hatching larvae of caenogastropods may also synthesize HCN, but a high rate of constitutive export of these molecules may preclude their accumulation within any subcellular compartment of the rhogocytes.

The foregoing assumes that rhogocytes in larvae of both *N. melanotragus* and caenogastropods synthesize HCN. Alternatively, in these two groups of larvae the different ultrastructural features of rhogocytes may reflect differing functions. Although rhogocytes in *N. melanotragus* may synthesize HCN, those of caenogastropod larvae may

synthesize another protein product. The coated vesicles associated with the subsurface cisternae of the caenogastropod larvae and the cisternae themselves contained material of the same appearance; therefore they may be importing materials from or exporting materials to the subsurface cisternae. Rhogocytes have been shown to selectively uptake molecules based on size (for example, Sminia, 1972; Skelding and Newell, 1975; Boer and Sminia, 1976); therefore it is possible that the vesicles are collecting material from the subsurface cisternae and transporting it into the cell for storage or breakdown. Lysosomal activity is common within the vesicles of rhogocytes (Sminia, 1972; Jones and Bowen, 1979) implying a degenerative function. Within the rhogocytes of *A. columbiana* and *M. stearnsii,* consistent with observations of Fioroni *et al.* (1984), there were vesicles being engulfed by electron dense vacuoles. This could be either for storage or degeneration within the vacuole. Therefore material within the subsurface cisternae and vesicles could be either waste products or material required for assembly of products within the rhogocytes.

4.2 Potential homology between rhogocytes and cyrtocytes

Cyrtocytes are the terminal cells of protonephridia, which are responsible for ultrafiltration of extracellular body fluid during the process of excretion and osmoregulation in animals that lack a blood vascular system (Ruppert and Smith, 1988). Podocytes are ultrafiltration cells in metanephridial systems, which also function for excretion and osmoregulation but only in animals that have a pressurized blood vascular system (Ruppert and Smith, 1988). The question of homology between rhogocytes,

cyrtocytes and podocytes arises due to the morphological similarities among these cells. Comparison of the larval rhogocytes in *A. columbiana, T. cancellata, M. stearnsii* and *N. melanotragus* with the cyrtocytes of *S. denticulata* showed that both exhibited sieve-like elaborations of the plasma membrane. In both cell types, the sieve structure was composed of cytoplasmic bars separated by slits with occluding diaphragms (for example, Figures 5 and 29). This is a unique and unusual morphological feature, which Haszprunar (1996) has argued is unlikely to have evolved independently in these cell types.

There were, however, differences between the sieve structures of rhogocytes and those of protonephridial cyrtocytes. The sieve complex of larval rhogocytes in the gastropod larvae described here overlaid subsurface cisternae, whereas the sieve of protonephridial cyrtocytes of *Siphonaria denticulata* opened into the cavity surrounding the cilia of the cell. This could however be interpreted as cyrtocytes having one large, ciliated subsurface cisterna. Another difference was that rhogocytes are solitary cells, as described previously (for example, Sminia, 1972; Fioroni *et al.*, 1984), whereas cyrtocytes are closely associated with cells of the nephridioduct of a protonephridium (Ruppert and Smith, 1988; Smith and Ruppert, 1988).

Rieger and Tyler (1979) extended Remane's (1952) homology theorem to establish criteria for evaluating homologous features of cellular ultrastructure. The two main criteria are: similarity in physical and temporal location of the structures being evaluated and the existence of structures with intermediate morphology. I have analyzed the potential homology of larval rhogocytes and terminal cells of larval protonephridia (cyrtocytes) in gastropod larvae according to these criteria.

I found that larval rhogocytes in larvae of three caenogastropods and a neritimorph occupy the same location as the cyrtocytes of heterobranch larvae. In all cases, these cells are located on either side of the esophagus at the level of the statocysts and cerebral ganglia (Figures 3, 10, 15, 20 and 27). Therefore, the first homology criterion, similarity in location, appears to be satisfied for rhogocytes and cyrtocytes in larval gastropods.

Intermediate structures are a second homology criterion, as their existence indicates a potential path of transformation between two cells or multicellular structures (Rieger and Tyler, 1979). However, at present, there are no cells in molluscs that show an intermediate structure between rhogocytes and cyrtocytes.

4.3 Potential size relationship

There are three major groups of gastropods that have a planktotrophic larval stage in their life history. These are: the Caenogastropoda, Heterobranchia, and Neritimorpha. Of these three, larvae produced by heterobranchs are generally smaller than those of neritimorphs and caenogastropods (Thorson, 1946; Scheltema, 1971; Ponder and Lindberg, 1997; Hadfield and Miller, 1982). The presence of rhogocytes in the planktotrophic larvae of three caenogastropods and a neritimorph, but not in a heterobranch larva, appears to be related to larval body size and presence of a definitive heart. A similar correlation exists between the occurrence of protonephridia and larval size. Specifically, small heterobranch larvae do not have rhogocytes but they do have protonephridia throughout the larval phase. Larvae of both caenogastropods and neritimorphs have rhogocytes, but they lack protonephridia. In caenogastropods,

protonephridia are present during the encapsulated embryonic period, but they are replaced by metanephridia at about the time of larval hatching (Ruthensteiner and Shaefer, 1991).

A correlation between organismal size and presence of protonephridia or metanephridia has also been documented for other bilaterians, particularly polychaete annelids. Ruppert and Smith (1988) have shown that small body size is typically associated with lack of a blood vascular system and these animals typically have protonephridia for osmoregulation and excretion. Protonephridia have terminal cells to perform the ultrafiltration step of primary urine formation. However, larger body size typically co-occurs with the presence of a blood vascular system. A pressurized blood vascular system is essential for the functioning of metanephridial systems because pressure filtration via podocytes accomplishes the ultrafiltration step of primary urine formation. Both caenogastropod larvae and neritimorph larvae have a blood vascular system pressurized by a beating heart during the entire interval of larval development (Ponder and Lindberg, 1997; Bandel *et al.*, 1997; Page and Ferguson, in preparation). It is therefore not surprising that these larvae have a metanephridium for excretion and osmoregulation. Alternatively, the relatively small heterobranch larvae do not have a pressurized blood vascular system until after metamorphosis. These larvae have protonephridia throughout the larval phase and replace these with a metanephridium only at metamorphosis (Page, 1994).

Although I found direct evidence for hemocyanin synthesis by rhogocytes only in young larvae of a neritimorph, I cannot exclude the possibility that the rhogocytes of caenogastropod larvae also synthesize HCN. If larval rhogocytes of both

caenogastropods and neritimorphs synthesize HCN, then the occurrence of these cells only in caenogastropods and neritimorphs may also relate to larval size. Hemocyanin is an oxygen-binding molecule that facilitates efficient uptake of environmental oxygen for delivery to tissues of an organism. Very small organisms, such as larvae of heterobranchs, may rely on diffusion for gas exchange rather than utilizing a transport pigment such as HCN.

4.4 Summary

Rhogocytes are a unique molluscan cell type that had not been previously described in planktotrophic larvae of members of this phylum. I identified rhogocytes within the planktotrophic larvae of three caenogastropods, *A. columbiana, T. cancellata* and *M. stearnsii* and a neritimorph, *N. melanotragus*, but rhogocytes were not present in larvae of the heterobranch *S. denticulata*. Further studies need to be undertaken to determine if this trend persists throughout other gastropods with planktotrophic larvae. These larvae should also be examined at different times throughout development to determine the exact time of the appearance of rhogocytes and to track how the rhogocytes change as the larvae approach and undergo metamorphosis. Monitoring how larval rhogocytes change throughout development may also give further insight into the function of these cells in larvae.

Based on previous literature on rhogocytes in adult molluscs, I hypothesized that rhogocytes functioned for synthesis of HCN. However, my observations provide evidence for HCN synthesis only in young larvae of *N. melanotragus*. Large stores of

HCN within the rhogocytes of *N. melanotragus* that had been recently released from their egg capsule may relate to a hypothesized period of intracapsular diapause.

Homology between rhogocytes and cyrtocytes of protonephridia cannot be excluded based on this study. TEM images are valuable in studying rhogocytes, however other tools such as *in situ* hybridization are necessary to gather more information on the characteristics of this cell and how it relates to other structurally similar cells including those of nephridial systems.

5.0 Literature Cited

Albrecht, U., Keller, H., Gebauer, W. and Markl, J. 2001. Rhogocytes (pore cells) as the site of hemocyanin biosynthesis in the marine gastropod *Haliotis tuberculata*. Cell and Tissue Research. 305: 455-462.

Anderson, D.T. 1962. The reproduction and early life histories of the gastropods *Bembicium auratum* (Quoy and Gaimard) (Fam. Littorinidae), *Cellana tramoserica* (Sower.) (Fam. Patellidae) and *Melanerita melanotragus* (Smith) (Fam. Neritidae). Proceedings of the Linnean Society of New South Wales. 87: 62-68.

Audesirk, G. and Audesirk, T. 1980. Complex mechanoreceptors in *Tritonia diomedea*. I. Responses to mechanical and chemical stimuli. Journal of Comparative Physiology. 141: 101–109.

Baeumler, N., Haszprunar, G. and Ruthensteiner B. 2011. Development of the excretory system in the polyplacophoran mollusc, *Lepidochitona corrugata*: The Protonephridia . Journal of Morphology. 272: 972-986.

Bandel, K., Riedel, F. and Weikert, H. 1997. Planktonic gastropod larvae from the Red Sea: a synopsis. Ophelia 47: 151-202.

Bartolomaeus, T. 1989. Larvale nierenorgane bei *Lepidochiton cinereus* (Polyplacophora) und *Aeolidia papillosa* (Gastropoda). Zoomorphology. 108: 297-307.

Berard, F., Blanco, P., Davoust, J., Neidhart-Berard, E.-M., Nouri-Shirazi, M., Taquet, N., Rimoldi, D., Cerottini, J.C., Banchereau, J. and Palucka, A.K. 2000. Cross-priming of naïve CD8 T cells against melonoma antigens using dendritic cells loaded with killed allogeneic melanoma cells. Journal of Experimental Medicine. 192(11): 1535-1543.

Bergmann, S., Lieb, B., Ruth, P. and Markl, J. 2006. The hemocyanin for a living fossil, the cephalopod *Nautilus pompilius*: protein structure, gene organization, and evolution. Journal of Molecular Evolution. 62: 362-374.

Beuerlein, K., Löhr, S., Westermann, B., Ruth, P. and Schipp, R. 2002b. Components of the cellular defense and detoxification of the common cuttlefish *Sepia officinalis* (Mollusca, Cephalopoda). Tissue and Cell. 34(6): 390-396.

Beuerlein, K., Ruth, P., Scholz, F.R., Springer, J., Lieb, B., Gebauer, W., Westermann, B., Schmidtberg, H., von Boletzky, S., Markl, J. and Schipp, R. 2004. Blood cells and the biosynthesis of hemocyanin in *Sepia* embryos. Micron. 35: 115-116.

Beuerlein, K., Ruth, P., Westermann, B., Löhr, S. and Schipp, R. 2002a. Hemocyanin and the branchial heart complex of *Sepia officinalis*: are the hemocytes involved in hemocyanin metabolism of coleoid cephalopods? Cell and Tissue Research. 310: 373-381.

Boer, H.H. and Sminia, T. 1976. Sieve structure of slit diaphragms of podocytes and pore cells of gastropod molluscs. Cell and Tissue Research. 170: 221-229.

Bonaventura, J. and Bonaventura, C. 1980. Hemocyanins: relationships in their structure, function and assembly. American Zoologist. 20: 7-17.

Cloney, R.A. and Florey, E. 1968. Ultrastructure of cephalopod chromatophore organs. Zeitschrift für Zellforschung und mikroskopische Anatomie. 89: 73–79.

Creese, R.G. 1980. Reproductive cycles and fecundities of two species of *Siphonaria* (Mollusca: Pulmonata) in south-eastern Australia. Australian Journal of Marine and Freshwater Research. 31(1): 37-47.

Dilly, P.N. and Messenger, J.B. 1972. The branchial gland: a site of haemocyanin synthesis in *Octopus*. Zeitschrift für Zellforschung und mikroskopische Anatomie. 132: 193-201.

Dolashka, P., Velkova, L., Illiev, I., Beck, A., Dolashki, A., Yossifova, L., Toshkova, R., Voelter, W. and Zacharieva, S. 2011. Antitumor activity of glycosylated molluscan hemocyanins via Guerin Ascites tumor. Immunological Investigations. 40: 130-149.

Ellerton, H.D., Ellerton, N.F. and Robinson, H.A. 1983. Hemocyanin – a current perspective. Progress in Biophysics and Molecular Biology. 41(3): 143-248.

Fahrner, A. and Haszprunar, G. 2001. Anatomy and ultrastructure of the excretory system of a heart-bearing and heart-less sacoglossan gastropod (Opisthobranchia, Sacoglossa). Zoomorphology. 121: 85-93.

Fioroni, V.P., Sundermann, G. and Scheidegger, D.P. 1984. Die Ultrastruktur der freien rhogocyten bei intrakapsulären veligern von *Nucella lapillus* (Gastropoda, Prosobranchia, Stenoglossa). Zoologischer Anzeiger. 212(3/4): 193-202.

Fretter, V. and Graham, A. 1994. British Prosobranch Molluscs. The Dorset Press, Dorchester, Dorset. pp. 422-427, 633.

Gittenberger, A. 2007. Recent population expansions of non-native ascidians in The Netherlands. Journal of Experimental Marine Biology and Ecology. 342: 122-126.

Goodrich, E.S. 1945. The study of nephridia and genital ducts since 1895. Quarterly Journal Microscopical Science. 86: 113-392.

Hadfield, M.G. and Miller, S.E. 1987. On developmental patterns of opisthobranchs. American Malacological Bulletin. 5: 197-214.

Hall, R.L., Pearson, J.S. and Wood, E.J. 1975. The haemocyanin of *Lymnaea stagnalis* L. (Gastropoda: Pulmonata). Comparative Biochemistry Physiology. 52B: 211-218.

Harris, J.R. and Markl, J. 1999. Keyhole limpet hemocyanin (KLH): a biomedical review. Micron. 30: 597-623.

Haszprunar, G. 1996. The molluscan rhogocyte (pore-cell, blasenzelle, cellule nucale), and its significance for ideas on nephridial evolution. Journal of Molluscan Studies 62: 185-211.

Helling, F. and Livingston, P.O. 1994. Ganglioside conjugate vaccines immunotherapy against tumors of neuroectodermal origin. Molecular and Chemical Neuropathology. 21: 299-309.

Helling, F., Zhang, S., Shang, A., Adluri, S., Calves, M., Koganty, R., Longenecker, B.M., Yao, T.-J., Oettgen, H.F. and Livingston, P.O. 1995. G_{M2}-KLH conjugate vaccine: increased immunogenicity in melanoma patients after administration with immunological adjuvant QS-21. Cancer Research. 55: 2783-2788.

Iveša, L., Chapman, M.G., Underwood, A.J. and Murphy, R.J. 2010. Differential patterns of distribution of limpets on intertidal seawalls: experimental investigation of the roles of recruitment, survival and competition. Marine Ecology Progress Series. 407:55-69.

Iyengar, E.V. 2005. Seasonal feeding-mode changes in the marine facultative kleptoparasite *Trichotropis cancellata* (Gastropoda, Capulidae): trade-offs between trophic strategy and reproduction. Canadian Journal of Zoology. 83: 1097-1111.

Jones, G.W. and Bowen, I.D. 1979. The fine structural localization of acid phosphatase in pore cells of embryonic and newly hatched *Deroceras reticulatum* (Pulmonata: Stylommatophora). Cell and Tissue Research. 204: 253-265.

Kano, Y. 2006. Usefulness of the opercular nucleus for inferring early development in neritimorph gastropods. Journal of Morphology. 267: 1120-1136.

Kano, Y., Chiba, S. and Kase, T. 2002. Major adaptive radiation in neritospine gastropods estimated from 28S rRNA sequences and fossil records. Proceedings of the Royal Society of London B. 269: 2457-2465.

Keller, H., Lieb, B., Altenhein, B., Gebauer, D., Richter, S., Stricker, S. and Markl, J. 1999. Abalone *(Haliotis tuberculata)* hemocyanin type 1 (HtH1) organization of

the ≈400kDa subunit, amino acid sequence of its functional units f, g and h. European Journal of Biochemistry. 264: 27-38.

Lesoway, M.P. and Page, L.R. 2008. Growth and differentiation during delayed metamorphosis of feeding gastropod larvae: signatures of ancestry and innovation. Marine Biology. 153: 723-734.

Lieb, B., Altenhein, B., Lehnert, R., Gebauer, W. and Markl, J. 1999. Subunit organization of the abalone *Haliotis tuberculata* hemocyanin type 2 (HtH2), and the cDNA sequence encoding its functional units d, e, f, g and h. European Journal of Biochemistry. 265: 134-144.

Lindberg, D.R. 2008. Patellogastropoda, Neritimorpha, and Cocculinoidea. In: Phylogeny and Evolution of the Mollusca. W.F. Ponder and D.R. Lindberg (eds.). University of California Press, Berkeley CA. pp. 271-296.

Manubens, A., Salazar, F., Haussmann, D., Figueroa, J., Del Campo, M., Martinez Pinto, J., Huaquin, L. Venegas, A., and Becker, M.I. 2010. *Concholepas* hemocyanin biosynthesis takes place in the hepatopancreas, with hemocytes being involved in its metabolism. Cell and Tissue Research. 342: 423-435.

Marigómez, I., Soto, M., Cajaraville, M.P., Angulo, E. and Giamberini, L. 2002. Cellular and subcellular distribution of metals in molluscs. Microscopy Research and Technique. 56: 358-292.

Markl, J., Lieb, B., Gebauer, W., Altenhein, B., Meissner, U. and Harris, J.R. 2001. Marine tumor vaccine carriers: structure of the molluscan hemocyanins KLH and HtH. Journal of Cancer Research and Clinical Oncology. 127(Suppl 2): R3-R9.

Markl, J., Savel-Niemann, A., Wegener-Strake, A., Süling, M., Schneider, A., Gebauer, W. and Harris, J.R. 1991. The role of two distinct subunit types in the architecture of keyhole limpet hemocyanin (KLH). Naturwissenchaften. 78: 512-514.

Martin, A.M., Martin, G.G., Butler, R. and Goffredi, S.K. 2011. Synthesis of keyhole limpet hemocyanin by the rhogocytes of *Megathura crenulata*. Invertebrate Biology. 130(4): 302-312.

Messenger, J.B., Muzii, E.O., Nardi, G. and Steinberg, H. 1974. Hemocyanin synthesis and the branchial gland of *Octopus*. Nature. 250: 154-155.

Miller, K.I. and van Holde, K.E. 1982. The structure of *Octopus dofleini* hemocyanin. Comparative Biochemistry and Physiology. 73B(4): 1013-1018.

Moreira, J., Chapman, M.G. and Underwood, A.J. 2006. Seawalls do not sustain viable populations of limpets. Marine Ecology Progress Series. 322: 179-188.

Page, L.R. 1994. The ancestral gastropod larval form is best approximated by hatching-stage opisthobranch larvae: evidence from comparative developmental studies. In: Reproduction and Development of Marine Invertebrates. W.H. Wilson, S.A. Stricker, and G.L. Shinn (eds.). John Hopkins University Press, Baltimore. pp. 206-223.

Page, L.R. 2002. Larval and metamorphic development of the foregut and proboscis in the caenogastropod *Marsenina (Lamellaria) stearnsii*. Journal of Morphology. 252: 202-217.

Page, L.R. and Parries, S.C. 2000. Comparative study of the apical ganglion in planktotrophic caenogastropod larvae: ultrastructure and immunoreactivity to serotonin. Journal of Comparative Neurology. 418: 383-401.

Parries, S.C. and Page, L.R. 2003. Larval development and metamorphic transformation of the feeding system in the kleptoparasitic snail *Trichotropis cancellata* (Mollusca, Caenogastropoda). Canadian Journal of Zoology. 81: 1650-1661.

Plummer, J.M. 1966. Collagen formation in Achatinidae associated with a specific cell type. Proceedings of the Malacological Society of London. 37: 189-197.

Ponder, W.F. and Lindberg, D.R. 1997. Towards a phylogeny of gastropod molluscs: an analysis using morphological characters. Zoological Journal of the Linnean Society. 119: 83-265.

Prince, J.S. and Johnson, P.M. 2006. Ultrastructural comparison of *Aplysia* and *Dolabrifera* ink glands suggests cellular sites of anti-predator protein production and algal pigment processing. Journal of Molluscan Studies. 72: 349-357.

Raven, C.P. 1966. Morphogenesis: The Analysis of Molluscan Development. International Series of Monographs in Pure and Applied Biology. Vol 2. J.E. Harris and E.W. Yemm (eds.). Pergamon Press Ltd., London. pp. 131-133, 164-168.

Remane, A. 1952. Die Grundlagen des natiirlichen Systems, der vergleichenden Anatomie und der Phylogcnctik. Akad. Verlagsges. Geest & Portig, Leipzig.

Richardson, K.C., Jarrett, L. and Finke E.H. 1960. Embedding in epoxy resins for ultrathin sectioning in electron microscopy. Stain Technology. 35: 313–323.

Rieger, R. and Tyler, S. 1979. The homology theorum in ultrastructural research. American Zoologist. 19(2): 655-666.

Risbec, J. 1932. Notes sur la ponte et le développement de mollusques gastéropodes de Nouvelle-Calédonie. Bulletin de la Société Zoologique de France. 57: 358-374.

Rivest, B.R. 1992. Studies on the structure and function of the larval kidney complex of prosobranch gastropods. Biological Bulletin. 182: 305-323.

Ruppert, E.E. 1994. Evolutionary origin of the vertebrate nephron. American Zoologist. 34(4): 542-553.

Ruppert, E.E. and Smith, P.R. 1988. The functional organization of filtration nephridia. Biological Reviews. 63: 231-258.

Ruth, P., Blum, W. and Bille, J. 1996. Immunocytochemical reaction of a haemocyanin antibody in the midgut gland of *Nautilus* (Cephalopoda, Tetrabranchiata). Experientia. 52: 549-553.

Ruth, P., Schipp, R. and Klüssendorf, B. 1988. Cytomorphology and copper content of the basal cells in the midgut gland of *Nautilus* (Cephalopoda, Tetrabranchiata). Zoomorphology. 108: 1-11.

Ruthensteiner B. and Schaefer, K. 1991. On the protonephridia and 'larval kidneys' of *Nassarius (Hinia) reticulata* (Linnaeus) (Caenogastropoda). Journal of Molluscan Studies. 57: 323-329.

Ryan, M., Terwilliger, N.B., Terwilliger, R.C. and Schabtach, E. 1985. Chiton hemocyanin structure. Comparative Biochemistry and Physiology. 80B(3): 647-656.

Scheltema, R.S. 1971. Larval dispersal as a means of genetic exchange between geographically separated populations of shoal-water benthic marine gastropods. Biological Bulletin. 140: 284-322.

Schmekel, L. and Weischer, M.L. 1973. Die blutdrüse der doridoidea (Gastropoda, Opisthobranchia) als ort möglicher hämocyanin-synthese. Zeitschrift fur Morphologie der Tiere. 76: 261-284.

Schnurr, M., Galambos, C., Scholz, F., Then, F., Dauer, M., Endres, S. and Eigler, A. 2001. Tumor cell lysate-pulsed human dendritic cells induce a T-cell response against pancreatic carcinoma cells: an *in vitro* model for the assessment of tumor vaccines. Cancer Research. 61: 6445-6450.

Seavy, D.K. 1977. Seasonal gametogenesis and egg laying in the prosobranch gastropods *Nucella lamellose, Nucella emarginata, Searlesia dira* and *Amphissa columbiana* on the Oregon coast. Ph.D. thesis. Oregon State University.

Skelding, J.M. and Newell, P.F. 1975. On the functions of the pore cells in the connective tissue of terrestrial pulmonate molluscs. Cell and Tissue Research. 156: 381-390.

Sminia, T. 1972. Structure and function of blood and connective tissue cells of the freshwater pulmonate *Lymnaea stagnalis* studied by electron microscopy and enzyme histochemistry. Zeitschrift fur Zellforschung und Mikroskopische Anatomie. 130: 497-526.

Sminia, T. and Boer, H.H. 1973. Haemocyanin production in pore cells of the freshwater snail *Lymnaea stagnalis*. Zeitschrift fur Zellforschung und Mikroskopische Anatomie. 145: 443-445.

Sminia, T. and Vlugt-van Daalen. 1977. Haemocyanin synthesis in pore cells of the terrestrial snail *Helix aspera*. Cell and Tissue Research. 183: 299-301.

Sminia, T., Boer, H.H. and Niemantsverdriet, A. 1972. Haemoglobin producing cells in freshwater snails. Zeitschrift fur Zellforschung und Mikroskopische Anatomie. 135: 563-568.

Smith, P.R. 1992. Polychaeta: Excretory system. In: Microscopic Anatomy of Invertebrates. Vol. 7. Annelida. F.W. Harrison and S.L. Gardiner (eds.). Wiley-Liss, Inc. New York. pp. 71-108.

Smith, P.R. and Ruppert, E.E. 1988. Nephridia. In: The Ultrastructure of the Polychaeta. W. Westheide and C.O. Hermans (eds.). Microfauna Marina. 4: 231-262.

Söhngen, S.M., Stahlmann, A., Harris, J.R., Müller, S.A., Engel, A. and Markl, J. 1997. Mass determination, subunit organization and control of oligomerization states of keyhole limpet hemocyanin (KLH). European Journal of Biochemistry. 248: 602-614.

Strathmann, M.F. 1987. Reproduction and Development of Marine Invertebrates of the Northern Pacific Coast. University of Washington Press, Seattle, London.

Streit, K., Jackson, D., Degnan, B.M. and Lieb, B. 2005. Developmental expression of two *Haliotis asinina* hemocyanin isoforms. Differentiation. 73: 341-349.

Tan, K.S. and Lee, S.S.C. 2009. Neritid egg capsules: are they all that different? Steentrupia. 30(2): 115-125.

Thorson, G. 1946. Reproduction and larval development of Danish marine bottom invertebrates; with special reference to the planktonic larvae in the Sound (Øresund). Meddelelser fra Kommissionen for Danmarks Fiskeri- og Havundersøgelser. Serie Plankton. 4: 1–523.

van Holde. 1997. Respiratory proteins of invertebrates: structure, function and evolution. Zoology. 100: 287-297.

van Holde, K.E., Miller, K.I. and Decker, H. 2001. Hemocyanins and invertebrate evolution. Journal of Biological Chemistry. 276(19): 15563-15566.

Wandall, H.H., Blixt, O., Tarp, M.A., Pederson, J.W., Bennett, E.P., Mandel, U., Ragupathi, G., Livingston, P.O., Hollingsworth, M.A., Taylor-Papadimitriou, J., Burchell, J. and Clausen, H. 2010. Cancer biomarkers defined by autoantibody signatures to aberrant O-glycopeptide epitopes. Cancer Research. 70(4): 1306-1313.

Wirguin, I., Suturkova-Milosević, L., Briani, C. and Latov, N. 1995. Keyhole limpet hemocyanin contains Gal(β1-3)-GalNAc determinants that are cross-reactive with the T antigen. Cancer Immunology, Immunotherapy. 40(5): 307-310.

Wolburg-Buchholz, K. 1972a. Blasenzellen im bindegewebe des schlundrings von *Cepaea nemoralis* L. (Gastropoda, Stylommatophora) I. Feinstruktur der zellen. Zeitschrift fur Zellforschung und Mikroskopische Anatomie. 128: 100-114.

Wolburg-Buchholz, K. 1972b. Blasenzellen im bindegewebe des schlundrings von *Cepaea nemoralis* L. (Gastropoda, Stylommatophora) II. Aufnahme und speicherung von ferritin. Zeitschrift fur Zellforschung und Mikroskopische Anatomie. 130: 262-278.

Wood, E.J., Corfield, G.C. and Siggens, K.W. 1981. Biosynthesis of haemocyanin in *Lymnaea stagnalis* L. (Gastropoda). Comparative Biochemistry and Physiology. 69B: 877-880.

Yonge, C.M. 1962. On the biology of the mesogastropod *Trichotropis cancellata* Hinds, a benthinc indicator species. Biological Bulletin. 122: 160-181.